Atmos. Chem. Phys. Discuss., 7, 10235–10285, 2007
www.atmos-chem-phys-discuss.net/7/10235/2007/

Atmospheric Chemistry and Physics Discussions

The high Arctic in extreme winters: vortex, temperature, and MLS and ACE-FTS trace gas evolution

G. L. Manney[1,2], W. H. Daffer[3], K. B. Strawbridge[4], K. A. Walker[5,6], C. D. Boone[6], P. F. Bernath[7,6], T. Kerzenmacher[5], M. J. Schwartz[1], K. Strong[5], R. J. Sica[8], K. Krüger[9], H. C. Pumphrey[10], L. Froidevaux[1], A. Lambert[1], M. L. Santee[1], N. J. Livesey[1], E. E. Remsberg[11], M. G. Mlynczak[11], and J. R. Russell III[12]

[1]Jet Propulsion Laboratory, California Institute of Technology, Pasadena, CA, USA
[2]New Mexico Institute of Mining and Technology, Socorro, NM, USA
[3]Columbus Technologies Inc., Pasadena, CA, USA
[4]Science and Technology Branch, Environment Canada, Ontario, Canada
[5]University of Toronto, Toronto, Ontario, Canada
[6]University of Waterloo, Waterloo, Ontario, Canada
[7]University of York, Heslington, York, UK
[8]University of Western Ontario, London, Ontario, Canada
[9]Leibniz-Institute for Marine Sciences at Kiel University (IFM-GEOMAR), Kiel, Germany
[10]University of Edinburgh, Edinburgh, UK
[11]NASA Langley Research Center, Hampton, Virginia, USA
[12]Hampton University, Hampton, Virginia, USA

Received: 21 June 2007 – Accepted: 2 July 2007 – Published: 17 July 2007

Correspondence to: G. L. Manney (manney@mls.jpl.nasa.gov)

Abstract

The first three Canadian Arctic Atmospheric Chemistry Experiment (ACE) Validation Campaigns at Eureka (80° N, 86° W) were during two extremes of Arctic winter variability: Stratospheric sudden warmings (SSWs) in 2004 and 2006 were among the strongest, most prolonged on record; 2005 was a record cold winter. New satellite measurements from ACE-Fourier Transform Spectrometer (ACE-FTS), Sounding of the Atmosphere using Broadband Emission Radiometry, and Aura Microwave Limb Sounder (MLS), with meteorological analyses and Eureka lidar and radiosonde temperatures, are used to detail the meteorology in these winters, to demonstrate its influence on transport and chemistry, and to provide a context for interpretation of campaign observations. During the 2004 and 2006 SSWs, the vortex broke down throughout the stratosphere, reformed quickly in the upper stratosphere, and remained weak in the middle and lower stratosphere. The stratopause reformed at very high altitude, above where it could be accurately represented in the meteorological analyses. The 2004 and 2006 Eureka campaigns were during the recovery from the SSWs, with the redeveloping vortex over Eureka. 2005 was the coldest winter on record in the lower stratosphere, but with an early final warming in mid-March. The vortex was over Eureka at the start of the 2005 campaign, but moved away as it broke up. Disparate temperature profile structure and vortex evolution resulted in much lower (higher) temperatures in the upper (lower) stratosphere in 2004 and 2006 than in 2005. Satellite temperatures agree well with Eureka radiosondes, and with lidar data up to 50–60 km. Consistent with a strong, cold upper stratospheric vortex and enhanced radiative cooling after the SSWs, MLS and ACE-FTS trace gas measurements show strongly enhanced descent in the upper stratospheric vortex during the 2004 and 2006 Eureka campaigns compared to that in 2005.

ACPD

7, 10235–10285, 2007

1 Introduction

The Atmospheric Chemistry Experiment (ACE) has been providing daily atmospheric measurements, with a particular focus on the polar winter middle atmosphere, since early 2004 (Bernath et al., 2005). The Canadian Arctic ACE Validation Campaigns (herein called Eureka campaigns) comprise an extensive set of ground-based measurements at the Polar Environment Atmospheric Research Laboratory (PEARL – formerly Environment Canada's Arctic Stratospheric Ozone (AStrO) Observatory) at Eureka (80.05° N, 273.6° E) during each late winter since the launch of ACE (e.g., Walker et al., 2005; Kerzenmacher et al., 2005). Data from the 2004 through 2006 campaigns are currently available and being used extensively for ACE validation. Together with the ACE-Fourier Transform Spectrometer (ACE-FTS), measurements from the Sounding of the Atmosphere using Broadband Emission Radiometry (SABER, since early 2002) and Aura Microwave Limb Sounder (MLS, since August 2004) instruments provide an unprecedented wealth of temperature and trace gas data covering the upper troposphere through the mesosphere for several years, enough to begin providing important advances in our ability to examine seasonal and interannual variability in meteorological conditions, transport and chemistry.

The winters of the first three Eureka campaigns (2003–2004, 2004–2005, and 2005–2006) provide an ideal "laboratory" for examining the extremes of Arctic winter middle atmosphere variability, including the effects of unusual meteorological conditions on transport and chemistry. A "major" stratospheric sudden warming (SSW) beginning in late December 2003 was the most prolonged on record (Manney et al., 2005); it was followed by recovery to an unusually strong vortex in the upper stratosphere, while the middle and lower stratospheric vortices remained very weak for the rest of the winter; the final warming was unusually late (Manney et al., 2005). The 2004–2005 winter was the coldest on record in the lower stratosphere (e.g., Manney et al., 2006b), with arguably the most chemical ozone (O_3) loss ever recorded in the Arctic (WMO, 2007, and references therein); the winter ended early in a major final warming. The 2005–2006

winter was similar in many ways to the 2003–2004 winter, with a very strong, prolonged major SSW beginning in early to mid January, a rapid recovery to an unusually strong vortex in the upper stratosphere while the lower and middle stratospheric vortices remained weak, and a very late final warming (e.g., Braathen et al., 2006; WMO, 2007; Manney et al., 2007b[1]). These three winters thus cover the extremes of recorded interannual variability in Arctic winter, and the ACE-FTS, MLS, and SABER data allow us to study them in a detail never before possible. The Eureka campaigns provide additional data for focusing in on local variations, including very high-resolution temperature data from lidar and radiosondes, and for intercomparison with and validation of the satellite data and recently upgraded meteorological analyses products.

In the following, we use the global daily temperature and trace gas data from MLS and SABER, along with ACE-FTS data and gridded meteorological analyses from operational assimilation systems, to contrast the meteorology of the upper troposphere through lower mesosphere in these winters. We focus on the meteorological conditions, using satellite data and meteorological analyses to provide context for and comparisons with high-resolution temperature measurements during the Eureka campaigns, and use MLS and ACE-FTS trace gas data to explore the implications of the extreme meteorological conditions for transport and chemistry in the high Arctic, especially over Eureka.

[1]Manney, G. L., Krüger, K., Pawson, S., Schwartz, M. J., Daffer, W. H., Livesey, N. J., Mlynczak, M. G., Remsberg, E. E., Russell III, J. M., and Waters, J. W.: The evolution of the stratopause during the 2006 major warming: Satellite Data and Assimilated Meteorological Analyses, J. Geophys. Res., submitted, available at http://mls.jpl.nasa.gov, 2007b.

2 Data descriptions

2.1 Eureka lidar temperature data

Environment Canada owns and operates a stratospheric ozone and temperature lidar, AStrO DIfferential Absorption Lidar (AStrO-DIAL) at PEARL. AStrO-DIAL has made measurements since 1993 focusing on the polar sunrise period. Carswell et al. (1996) give a detailed description of the instrument, which uses a XeCl Excimer laser (Lumonics 600) with 50 W output power at 308 nm (300 Hz), and a hydrogen Raman cell to convert some of the energy to 353 nm. The data acquisition system provides five minute averaged profiles with different chopper and filter combinations (to minimize non-linearity effects in the photomultiplier tubes and screen out optically thick cloud events); these profiles are pasted together and averaged to provide nightly profiles with 300 m vertical resolution. Rayleigh temperature profiles are calculated at 353 nm (which is much less sensitive to ozone absorption than the 308 nm channel) using the ideal gas law and assuming hydrostatic equilibrium as described by Hauchecorne and Chanin (1980). A constant initial temperature seed at 70 km of 220 K has been used in the first temperature profile retrievals shown here. A final calibration factor is applied based on temperature data from the top three kilometres of Eureka radiosonde (Sect. 2.2) profiles. Lidar temperature profiles typically extend below 30 km, depending on aerosol/cloud conditions. Previous studies (e.g. Gross et al., 1997) indicate that choosing an incorrect initial seed affects the final profile significantly only in the top ~10–15 km; below that, sensitivity tests for AStrO-DIAL temperatures show an error in the temperature profile of $\lesssim$1 K for a 10–20 K error in the seed. The statistical error in the temperature profiles shown here above ~50 km altitude can be significant (~20 K) due to the limited statistics from the low signal strength. As shown by Duck and Greene (2004, and references therein), even at the highest altitude, lidar temperature profiles can capture gravity waves and other small vertical scale structure that is absent in lower resolution profiles from satellites.

ACPD
7, 10235–10285, 2007

EGU

2.2 Eureka radiosonde temperature data

Radiosonde measurements at Eureka (location: 79.99 N, 85.94 W, 10 m/MSL) are from sondes launched operationally by Environment Canada (EC) at 11:15 and 23:15 UT each day; data from the 11:15 launches are shown here. Detailed information on the radiosondes is provided by Vaisala from the World Meteorological Organization (WMO) International Radiosonde Comparisons (Nash and Schmidlin, 1987; Ivanov et al., 1991). These radiosondes are Vaisala RS80, using a hydrogen filled balloon. The ascent rates of the balloons are ∼5 m/s and typical maximum heights are ∼30 km. Measurements taken are time, pressure, temperature, relative humidity, dew point temperature, wind speed and wind direction. Pressure and temperature are measured using capacitive sensors. The pressure (range: 1060 hPa to 3 hPa, resolution: 0.1 hPa) is measured with an aneroid capsule which changes a capacitor. These changes are recorded and converted into pressure. The temperature (range: +60C to –90C, resolution: 0.1 K) is measured with a chip of ceramic dielectric placed between two electrodes; the capacitance between the electrodes changes with temperature. Vaisala's specification for the time constant is 2.5 s. The data, transmitted by radio signals, are smoothed by the ground station equipment to a 10 s temporal resolution resulting in a vertical resolution of ∼50 m.

2.3 ACE-FTS data

SCISAT-1, the satellite carrying the ACE mission (Bernath et al., 2005) was launched August 2003. The primary instrument is the ACE-FTS, a Fourier transform spectrometer featuring high resolution (0.02 cm^{-1}, corresponding to a ±25 cm maximum optical path difference) and broad spectral coverage in the infrared (750–4400 cm^{-1}). ACE-FTS works primarily in the solar occultation mode, collecting atmospheric limb measurements using the sun as a radiation source. Latitudes of ACE-FTS measurements vary over an annual cycle with coverage as high as ±85° and an emphasis on the polar regions in winter and spring; vertical resolution is ∼3–4 km. Version 2.2 (including

ACPD
7, 10235–10285, 2007

updates for O_3, H_DO and N_2O_5) of the ACE-FTS retrievals (Boone et al., 2005) is used here. ACE-FTS temperatures are retrieved only above 12 km; below that they are constrained to values from Canadian Meteorological Center (CMC) analyses. Temperature precision is typically ~2–4 K through the stratosphere, and ~4–7 K in the mesosphere. Initial validation studies using ACE-FTS version 1.0 temperatures showed agreement to within ~2.5 K or better with correlative measurements from 10–45 km (McHugh et al., 2005; Kerzenmacher et al., 2005; Froidevaux et al., 2006). ACE-FTS v2.2 temperatures are validated by Sica et al. (2007)[2]. Initial validation of v1.0 ACE-FTS temperature and trace gases was presented in a 2005 special section of Geophysical Research Letters (e.g., Walker et al., 2005; McHugh et al., 2005; Petelina et al., 2005; Fussen et al., 2005; Mahieu and Fels, 2005; Jin et al., 2005; Clerbaux et al., 2005). Detailed validation studies of the baseline ACE-FTS v2.2 trace gases, including CO (Clerbeaux et al., 2007[3]) and H_2O (Carleer et al., 2007[4]) are presented in papers in this special issue of Atmospheric Chemistry and Physics.

2.4 Aura MLS data

MLS measures millimeter- and submillimeter-wavelength thermal emission from the limb of Earth's atmosphere. Detailed information on the measurement technique and the Aura MLS instrument is given by Waters et al. (2006). The Aura MLS fields-of-view point in the direction of orbital motion and vertically scan the limb in the orbit plane, leading to data coverage from 82° S to 82° N latitude on every orbit. Vertical profiles are measured every 165 km along the suborbital track.

[2]Sica, R. J., Izawa, M., Petelina, S. V., et al.: Validation of ACE temperature using ground-based and space-based meassurements, Atmos. Chem. Phys. Discuss., in preparation, 2007.

[3]Clerbaux, C., George, M., Walker, K. A., et al.: CO measurements from the ACE-FTS mission: Validation using ground-based, airbourne and satellite observations, Atmos. Chem. Phys. Discuss., in preparation, 2007.

[4]Carleer, M., Boone, C. D., Walker, K. A., et al.: ACE-FTS water vapor validation, Atmos. Chem. Phys. Discuss., in preparation, 2007.

The initial public release of MLS data was version 1.5 (v1.5). Reprocessing with MLS v2.2 will take over a year to complete, but the subset that has been reprocessed includes most days in the 2005 and 2006 Eureka campaigns. We use v1.5 data for overviews covering the full winters; initial v1.5 validation comparisons are given by Froidevaux et al. (2006) and Barrett et al. (2006). MLS v1.5 temperatures show a small high bias with respect to many correlative measurements in the middle and lower stratosphere, and alternating high and low biases in the upper stratosphere (Livesey et al., 2005; Froidevaux et al., 2006; Schwartz et al., 2007[5]). Vertical resolution of the Aura MLS v1.5 data is ∼3–4 km in the lower and middle stratosphere, depending on the product (Froidevaux et al., 2006; Livesey et al., 2005, available from the MLS web site, http://mls.jpl.nasa.gov); for v1.5 temperature, the vertical resolution is ∼7–8 km in the upper troposphere/lower stratosphere, ∼4 km in the stratosphere, and ∼6–9 km near the stratopause and in the lower mesosphere. The precision of MLS v1.5 temperatures is typically near 1 K in the stratosphere.

For comparisons and displays focusing on the Eureka campaign periods, we use MLS v2.2 data. Schwartz et al. (2007)[5] validated v2.2 temperature. Vertical resolution is ∼5 km in the upper troposphere and near the tropopause, ∼4 km in the stratosphere, and ∼8–9 km near the stratopause and in the lower mesosphere; precision is better than ∼1 K through the upper stratosphere, degrading to 2–2.5 K above that (Schwartz et al., 2007[5]). Detailed validation of MLS trace gases shown here is given in other papers for the special section of Journal of Geophysical Research-Atmospheres on Aura validation: Lambert et al. (2007)[6] (N_2O and H_2O), Froidevaux et al. (2007b[7],

[5]Schwartz, M. J., Lambert, A., Manney, G. L., et al.: Validation of the Aura Microwave Limb Sounder temperature and geopotential height measurements, J. Geophys. Res., submitted, available at http://mls.jpl.nasa.gov, 2007.

[6]Lambert, A., Read, W. G., Livesey, N. J. , et al.: Validation of the Aura Microwave Limb Sounder stratospheric water vapor and nitrous oxide measurements, J. Geophys. Res., submitted, available at http://mls.jpl.nasa.gov, 2007.

[7]Froidevaux, L., Jiang, Y. B., Lambert, A., et al.: Validation of EOS MLS stratospheric ozone

and references therein) (O_3), Froidevaux et al. (2007a)[8] (HCl), Santee et al. (2007b)[9] (HNO_3), and Pumphrey et al. (2007)[10] (CO). These papers validate version 2.2 (v2.2) MLS data and discuss changes from version 1.5 (v1.5).

Quality control recommendations given in Livesey et al. (2005) (for v1.5) and in the Aura Validation Issue papers are used to screen the MLS data.

2.5 SABER data

The Sounding of the Atmosphere using Broadband Emission Radiometry (SABER) (Mlynczak and Russell, 1995) instrument, launched on the Thermosphere Ionosphere Mesosphere Energetics and Dynamics satellite in December 2001, measures profiles of kinetic temperature using 15-μm and 4.3-μm CO_2 limb-emission radiance measurements. Pressure is measured from spectral contrast and temperature is then inferred from pressure and pointing heights assuming hydrostatic equilibrium. The effective vertical resolution of SABER temperature is ~2 km although it is retrieved on a higher-resolution fixed set of pressure surfaces (Remsberg et al., 2003). Version 1.06 (v1.06) SABER temperatures are used here. Precision of the SABER temperatures is of order 1 K or better in the stratosphere, but becomes somewhat larger (~1.5 K) by the middle mesosphere. Test days of the Version 1.06 (v1.06) SABER temperatures compare very well with correlative profiles and with profiles from the Upper Atmosphere Research Satellite (UARS) HALOE (see also Remsberg et al., 2002). Non-local-thermodynamic

measurements, J. Geophys. Res., submitted, available at http://mls.jpl.nasa.gov, 2007b.

[8] Froidevaux, L., Jiang, Y. B., Lambert, A., et al.: Validation of EOS MLS HCl measurements, J. Geophys. Res., submitted, available at http://mls.jpl.nasa.gov, 2007a.

[9] Santee, M. L., Lambert, A., Read, W. G. , et al.: Validation of the Aura Microwave Limb Sounder HNO_3 measurements, J. Geophys. Res., submitted, available at http://mls.jpl.nasa.gov, 2007b.

[10] Pumphrey, H. C., Filipiak, M. J., Livesey, N. J., et al.: Validation of the Aura Microwave Limb Sounder stratospheric and mesospheric CO measurements, J. Geophys. Res., submitted, available at http://mls.jpl.nasa.gov, 2007.

equilibrium effects in the very cold conditions (∼130 K) of the summer polar mesopause (near 85 km) are not modeled well in SABER v1.06, leading to a mesopause that is ∼3 km too low compared to climatological and falling spheres data (Kutepov et al., 2006); that discrepancy has been corrected in v1.07. The v1.06 bias in that region is not a factor for the wintertime conditions shown here.

2.6 Meteorological datasets

The Goddard Earth Observing System Version 4.03 (GEOS-4) analyses are the primary gridded meteorological dataset shown here. Some individual profile comparisons also show GEOS-5, Met Office (MetO) and European Centre for Medium-Range Weather Forecasts (ECMWF) analyses. Manney et al. (2007b)[1] show temperature comparisons between GEOS-4, GEOS-5 and ECMWF during the 2005-2006 Arctic winter. Each of the analyses is briefly described below.

The GEOS-4 analyses are described by Bloom et al. (2005); the assimilation procedure uses a Physical Space Statistical Analysis Scheme. The GEOS-4 data are provided on 55 hybrid (σ/pressure) model levels from the surface to 0.01 hPa. The horizontal grid is 1.0° latitude by 1.25° longitude; six-hourly average fields are provided centered at 00:00, 06:00, 12:00 and 18:00 UT. Besides the standard meteorological variables, GEOS-4 products include PV calculated internally in the model.

GEOS-5 analyses (Reinecker et al., 2007) have been produced for the period of the Aura mission, from August 2004 through the present, and have now replaced GEOS-4 as the ongoing operational system. GEOS-5 uses the Gridpoint Statistical Analysis method of Wu et al. (2002), a 3D-Var system, and a six-hour analysis window. GEOS-5 analyses are provided on 72 model levels from the surface to 0.01 hPa, and a 0.5° latitude by 2/3° longitude grid.

The MetO data through 12 March 2006 are from the stratosphere-troposphere data assimilation system first developed for the UARS project (Swinbank and O'Neill, 1994), and have been produced since October 1991. The system now uses a three-dimensional variational (3D-Var) scheme (Lorenc et al., 2000) that was implemented in

late 2000, and a dynamical core (Davies et al., 2005) implemented in late 2003 (Swinbank et al., 2002, 2004). These MetO data are supplied once-daily at 12:00 UT on a 2.5° latitude by 3.75° longitude grid, at 6 levels per decade in pressure between 1000 and 0.1 hPa. After 12 March 2006, the stratospheric analyses are provided from the same numerical weather prediction (NWP) model system as operational forecasts from the MetO (Walters et al., 2007[11]), on a 0.375° latitude by 0.5625° longitude grid, at 27 levels from 1000 to 0.4 hPa.

The ECMWF assimilation is a 4D-Var system based on a spectral GCM (e.g., Simmons et al., 2005). Operational ECMWF data shown here are from the T799/91-level system with a top at 0.01 hPa that became operational in February 2006 (e.g., Untch et al., 2006, available at http://www.ecmwf.int/publications/newsletters/). Model level data from the T799/91-level system are used at levels up to 0.01 hPa for profile comparisons. The T799/91-level data were extracted on a 2.5°×2.5°horizontal grid.

2.7 Data handling for Eureka and ACE-FTS comparisons

For examination of data at specific locations, either at Eureka or those coincident with ACE-FTS measurements, gridded meteorological analyses and products derived from them are interpolated bi-linearly to the locations in question. For ACE-FTS and some Eureka comparisons, pre-calculated "Derived Meteorological Products" (DMPs) are available from MetO, GEOS-4, and GEOS-5 analyses (Manney et al., 2007a[12]).

For Eureka comparisons and overviews, all MLS and SABER profiles taken on the same day within 2° latitude and 8° longitude of Eureka are used. The same criteria are applied to determine if an ACE-FTS profile is coincident with Eureka. For ACE-FTS and SABER, this is no more than one profile per day; for MLS, it is typically four to

[11] Walters, D., Earnshaw, P., Milton, S., et al.: Enhancing Vertical and Horizontal Resolution in the Met Office Global NWP (Unified) Model, in preparation, 2007.

[12] Manney, G. L., Daffer, W. H., Zawodny, J. M., et al.: Solar Occultation Satellite Data and Derived Meteorological Products: Sampling Issues and Comparisons with Aura MLS, J. Geophys. Res., submitted, available at http://mls.jpl.nasa.gov, 2007a.

eight profiles per day, which are averaged (with each given equal weight) to get the daily profiles shown. The same geographic criteria are used to determine whether a SABER or MLS profile is coincident with ACE-FTS, but data are constrained to within 12 hours before or after each ACE-FTS measurement; again, MLS profiles coincident with an ACE-FTS occultation are averaged to get a single profile for each day.

3 The 2004, 2005 and 2006 late winters at Eureka

3.1 Synoptic context

Figures 1 through 3 show maps of scaled potential vorticity (sPV; in "vorticity units", Dunkerton and Delisi, 1986; Manney et al., 1994) in the upper, middle and lower stratosphere, respectively. The same three days, chosen during the Eureka campaigns and to coincide with specific comparisons shown below, are described in each year, to contrast the meteorological conditions. Locations of Eureka and of ACE-FTS measurements are indicated.

After the major warmings in January 2004 and 2006, the upper stratospheric vortex (Fig. 1) redeveloped to be unusually large and strong by 24 February (Fig. 1); in contrast, in 2005, the upper stratospheric vortex had weakened by this time (as is more common for late February) and was distorted and shifted off of the pole by strong wave activity leading to the final warming. By 6 March, the 2004 and 2006 upper stratospheric vortices were still very strong, while the 2005 vortex was breaking down at the start of the major final warming and moved away from Eureka as it decayed. By 18 March 2005, the vortex breakup had progressed so that there was an anticyclone (low sPV) over the pole with an elongated vortex remnant surrounding it. The 2004 and 2006 vortices were still strong and positioned over Eureka on 18 March, but had started to weaken and shrink. The upper stratosphere thus presents an apparently contrary picture in the high Arctic in February and March, wherein the so-called warm, disturbed years had colder, stronger vortices than the "unusually cold" year.

In the middle stratosphere (Fig. 2), the 2004 and 2006 vortices were still recovering and strengthening slowly after the prolonged SSWs during 24 February through 18 March; the vortex redeveloped more strongly in 2004 than in 2006, such that during the early part of the 2006 Eureka campaign, the middle stratospheric vortex was still very weak; in both years, the vortex was over Eureka in March, with lowest temperatures over the pole, and the vortex edge over Eureka in late February. During the 2005 campaign, the vortex was weakening and shifted off the pole as the major final warming started – that SSW qualified as major (that is, easterly winds north of 60° N down to 10 hPa) on 10 March 2005. By 18 March 2005, the final warming had progressed so that a large, elongated vortex remnant was located well off the pole equatorward of 60° N, and high temperatures were over the pole (and Eureka). Thus, like the upper stratosphere, the Arctic during the period of the Eureka campaigns in the disturbed 2004 and 2006 winters had a stronger, colder, more pole-centered vortex than the overall much colder 2005 winter.

In the lower stratosphere (Fig. 3), because radiative cooling is much slower and the effects of the SSW propagate down later, the 2004 and 2006 vortices never recovered substantially more after the SSWs. The 2006 vortex in late winter was even smaller and weaker than that in 2004. In 2005, the lower stratospheric vortex was strong, but distorted and variable throughout the winter (e.g. Manney et al., 2006b), as seen here on 24 February and 6 March. By 18 March 2005, with the major final warming in progress, the vortex was becoming even more active; a few days after this, it broke into two fragments and continued to decay. The vortex edge was over Eureka in 2005 until ~8 March 2005.

3.2 Overview from MLS, SABER, and meteorological analyses

An overview of the temperature evolution in relation to the vortex at Eureka is shown in Fig. 4, using temperatures from MLS and SABER measurements coincident with Eureka and from GEOS-4 analyses interpolated to Eureka's location. The sPV contours demark the position of the vortex edge in the stratosphere (~200–0.7 hPa). In the early

winter, Eureka was well inside the vortex in each year (black contour farther into the vortex was last to pass over Eureka). In the cold 2004–2005 winter, with no strong midwinter SSWs, the vortex remained over Eureka until late February to early March (depending on the altitude) when it began its early springtime breakup. The decreasing sPV values (black, then white contour over Eureka) show the vortex edge crossing Eureka's location as it moved away from the pole during its final breakup. In 2003-2004, the prolonged major SSW began in late December, at which time the vortex moved away from Eureka. Similar behavior was seen in 2005–2006, but beginning in early to mid-January. In these years, a pole-centered upper stratospheric vortex redeveloped strongly and quickly after the SSW (cf. Fig. 1), remaining over Eureka for the duration of the 2004 and 2006 validation campaigns. That the sPV contours suggest extravortex air over Eureka in the lower stratosphere during the campaigns does not necessarily indicate a vortex located away from Eureka, but reflects how weak and ill-defined the vortex was during these periods. Thus, because of the different extremes in the meteorological conditions, the Eureka campaigns in 2004 and 2006 were conducted within the Arctic vortex at altitudes where it had redeveloped, while that in 2005 was conducted primarily outside or at the edge of the vortex.

The sPV scaling used becomes inappropriate near the stratopause, since the static stability there becomes very different from the value assumed in the PV scaling; the contours shown typically lie just below the stratopause as defined by the temperature maximum, and thus provide another indication of the stratopause altitude. In early winter in each year, the stratopause at Eureka lies near 55–60 km, consistent with previous studies (e.g., Hitchman et al., 1989) that show it to be at higher altitude and separated from the midlatitude stratopause as a result of gravity wave driven processes. In 2004-2005, the stratopause altitude remains near that level throughout the winter, dropping slightly in spring, and its position as represented in MLS, SABER and GEOS-4 agrees well. As reported by Manney et al. (2007b)[1], during the 2006 major SSW, the stratopause dropped to near 30 km and then became ill-defined in late January; similar behavior has been seen during previous strong SSWs (Labitzke, 1972).

In early February, it reformed at very high altitude, near 80 km over Eureka, and began dropping and warming rapidly during the strong vortex recovery in the upper stratosphere/lower mesosphere. Siskind et al. (2007) showed model simulations indicating that the very high stratopause in early February 2006 resulted from filtering by the disturbed stratospheric flow at lower altitudes of gravity waves that would normally break near 50 km, and that are critical in determining the climatological polar stratopause structure (Hitchman et al., 1989; Siskind et al., 2007, and references therein). The 2006 Eureka campaign began just after the reformation of the stratopause at very high altitude. As discussed by Manney et al. (2007b)[1], GEOS-4 and other operational analyses, which are not constrained by data above ~50 km, and use models with tops no higher than 0.01 hPa (near 80 km), underestimate the variations in stratopause altitude, and show it reforming much too low. The SABER data in 2004 don't cover the Arctic during the SSW or at the beginning of the recovery, but suggest very similar behavior during the 2003–2004 winter.

The evolution of the coldpoint, the temperature minimum in the stratosphere, is quite distinct from that of the tropopause (the latter is the shallow local minimum near 250–400 hPa seen best in GEOS-4). During most of the cold 2004–2005 winter, and before the SSWs in 2004–2005 and 2005–2006, the deepest temperature minimum is between 100 and 30 hPa. After the SSWs started in 2004 and 2006, that temperature minimum became very shallow and dropped in altitude. As the stratopause reformed at very high altitude, a strong temperature minimum formed below it near 3 hPa (~45 km) and gradually moved down. Thus the coldpoint was near 10–3 hPa during the 2004 and 2006 Eureka campaigns, but near 30–60 hPa in 2005. We detail stratopause and tropopause evolution more quantitatively below.

Figure 5 shows the time evolution of the stratopause at Eureka from MLS, SABER and GEOS-4. While GEOS-4 cannot accurately capture the stratopause behavior during the aftermath of the 2004 and 2006 SSWs, it does capture the behavior in 2006 fairly accurately as the stratopause drops and cools during the SSW, suggesting that it gives a reasonable representation of that period in 2004, when MLS had not yet

been launched and SABER was viewing high southern-hemisphere latitudes. Before and during the major SSWs, and throughout the 2004–2005 winter, the GEOS-4 stratopause is slightly warm compared to the satellite data, becoming much too warm during the reformation after the 2004 and 2006 SSWs, even after the stratopause has dropped to typical altitude and its position is once again accurately captured by GEOS-4. MLS and SABER stratopause altitudes and evolution agree very well; when the stratopause altitude is very high after the 2006 SSW, MLS temperatures are slightly lower than SABER, whereas when it is near 50–60 km in 2005 and after it has dropped in 2006 MLS temperatures tend to be slightly higher. Froidevaux et al. (2006) showed MLS v1.5 global-mean temperatures to be biased high with respect to several correlative datasets below ∼2 hPa and low above ∼0.4 hPa, consistent with this evolution of biases; the coarsening MLS vertical resolution at higher altitude may also tend to result in an underestimate of stratopause temperature at higher altitude.

The evolution of the tropopause is shown in Fig. 6 using GEOS-4 analyses. Because the analyses are quite well-constrained by data below ∼10 hPa, and the atmospheric processes parameterized in the models are better understood than those near and above the stratopause, GEOS-4 should provide an accurate picture of this region (also see radiosonde comparisons below, Sect. 3.4). SABER measurements do not, and MLS often do not, extend low enough to capture the polar winter tropopause. We show the tropopause calculated from the WMO (temperature gradient) definition, using the algorithm of Reichler et al. (2003), and a "dynamical" definition using the 3.5 PVU PV contour (which Highwood and Berrisford, 2000 and Schoeberl, 2004 have shown to be appropriate for the extratropics); the coldpoint is also shown. The search for a tropopause is halted if it is not found at a pressure higher than 10 hPa (altitude less than ∼30 km); the search for the coldpoint extends to 1 hPa. The WMO and dynamical tropopause altitudes and temperatures agree quite well throughout, and the PV at the WMO tropopause typically ranges from ∼2 to ∼5 PVU, fairly symmetrically around the dynamical value; the tropopause thus defined coincides with the shallow temperature minimum near 250–400 hPa (5–8 km) mentioned above. In contrast (note radically

ACPD
7, 10235–10285, 2007

EGU

different altitude scales), the coldpoint value varies from ~8 to over 40 km in 2004 and 2006. During 2004 and 2006, the temperature minimum is near 3 hPa at the beginning of the recovery from the SSWs, during the first part of the Eureka campaigns, dropping to near 10 hPa (~30 km) in March. During most of the 2005 winter, the coldpoint was near 20–25 km and up to ~25 K colder than the tropopause. After the final warming in 2005, the coldpoint coincided with the WMO and dynamical tropopauses. As shown in more detail below (Sects. 3.3 and 3.4), the variations in temperature extrema in the winters with prolonged SSWs are reflected in very unusual temperature profiles throughout the stratosphere.

While tropopause variations during the SSWs are not as dramatic as those of the stratopause, the tropopause at Eureka was distinctly higher and colder in the 2004–2005 winter than the other two winters. Day-to-day variations dominate the variability, but it appears that the tropopause at the very high latitude of Eureka drops and warms during the SSWs, at the same time the stratopause is dropping and cooling. Examination of hemispheric tropopause structure (not shown) indicates a higher, colder tropopause prior to the SSWs at lower latitudes, near ~60° N, consistent with forcing of the warming related to upper tropospheric wave activity.

We show below detailed comparisons of temperatures from satellites, analyses, and ground-based data during the Eureka campaigns. These provide a close-up view of the striking differences in meteorological conditions in the high Arctic between the warmest and the coldest Arctic winters, and how those conditions can affect interpretation of the Eureka data.

3.3 Comparisons with Eureka lidar

Figures 7 through 9 show selected lidar temperature profiles recorded at Eureka during the three winters, compared with MLS (2005 and 2006), SABER, ACE-FTS and GEOS-4, GEOS-5 (2005 and 2006) and ECMWF (2006) analyses. There is quite good agreement between the lidar profiles and those from each of the satellite instruments below ~55–60 km (0.1 to 0.2 hPa), sometimes higher, while the meteorological anal-

yses generally have trouble capturing the behavior above ~1 hPa (and, indeed, often do not even show a consensus there), especially in February 2004 and 2006. During these same periods, when the stratopause is very high, the lidar profiles tend to show a stratopause that is too low and too cold compared to the satellite instruments. Other departures of the lidar profiles from the satellite measurements and/or the analyses above 1 hPa are seen, and many of these can be explained by variations in atmospheric conditions, as discussed below.

Comparing the profiles in February of 2004, 2005 and 2006 shows the striking difference in temperature structure at Eureka for the two types of extreme conditions represented in these winters: In 2005, the profiles show a broad temperature minimum between ~300 and 30 hPa, and a sharp temperature maximum near 1 to 0.3 hPa; this is a characteristic wintertime temperature structure in the Arctic. In contrast, in February 2004 and 2006, there was a shallow temperature minimum near 300–400 hPa, followed by a gradual decrease in temperature up to 3 to 1 hPa, with a strong temperature maximum at or above 0.01 hPa. Thus, the conditions during the recovery from the prolonged SSWs led to temperatures that decreased with altitude through most of the stratosphere (commonly defined as the region where temperature increases with altitude).

In late February 2004, on each of the days shown, the lidar profiles show a notch near or just below the stratopause that is apparent in the SABER and/or ACE-FTS profiles on some days, but not on others; the GEOS-4 analyses show no sign of this feature. Figure 10 (left panels) shows cross-sections of SABER and GEOS-4 temperature at 80° N on 25 February 2004, with the longitude of Eureka indicated. On this day, when SABER captures the notch shown in the lidar profile, there is, in fact, a double-peak in stratopause temperature extending over Eureka; GEOS-4 does not represent the stratopause well at this time (cf., Fig. 4). Note also that Eureka is at the edge of a region with very strong gradients in stratopause temperature and altitude. Examination of cross-sections for surrounding days shows a similar pattern, with small variations in the positions of the stratopause double-peak and gradients with respect to Eureka.

ACPD
7, 10235–10285, 2007

This suggests that these are real atmospheric features with small horizontal extent such that they may be captured by some but not other instruments on any given day. On the same day, there is a notch in the lidar and GEOS-4 profiles just below 1 hPa that does not appear in the SABER profile. We see in Fig. 10 how this arises from a double-minimum in temperature in the GEOS-4 profile, which is not represented in SABER. Thus, the lidar observations lend support to the possibility that GEOS-4 may be capturing a real atmospheric feature that has been missed by SABER (which has quite coarse horizontal measurement spacing). A similar feature, with a similar origin, is seen on 4 March 2004 in lidar and GEOS-4 profiles (Fig. 10, right panels). Note that on 4 March, the gradients in stratopause altitude near Eureka are much smaller than on 24 February, but temperatures still show strong local variations. Consistent with this, the stratopause altitude in the lidar profile appears to agree well with that in SABER and ACE-FTS, but the lidar shows lower maximum temperatures.

On 6 March 2005, a sharp temperature maximum near 0.03 hPa is seen in the lidar profile, but not in MLS or SABER. There is a slight suggestion of a maximum in the ACE-FTS profile, and an indication of a corresponding maximum in GEOS-4 and GEOS-5. Figure 11 (left panels) shows cross-sections of MLS, SABER and GEOS-4 temperatures. All show a double-peak in the temperature profile, but its upper branch extends farther across Eureka in GEOS-4 than in MLS and SABER; thus it is plausible that the high horizontal resolution of GEOS-4 may be allowing it to model a feature that is not fully captured by the coarser spatial sampling of MLS and SABER. Eureka is also at a location of strong temperature gradients near the temperature minimum between 100 and 10 hPa, which could account for the higher temperatures in the lidar profile there. On 25 February 2006 (Figs. 9 and 11, right panels), there is an oscillation in the MLS temperature profile near 1 hPa that seems to be echoed in the analysis profiles (especially ECMWF), but not in either SABER or the lidar profile. Thus, in this case, the lidar does not provide evidence of atmospheric origin; since both assimilated products and MLS can contain unrealistic vertical oscillations, the veracity of the feature remains unclear.

The lidar profile on 25 February 2006 (Fig. 9) is an example where the lidar stratopause appears too low and too cool compared to the satellite data; such cases are common in 2006 and in 2004 (the latter especially in the earlier, February, measurements). Figure 11 (right panels) shows no obvious indication in the conditions surrounding Eureka of an atmospheric reason for this. Examination of all seven individual MLS profiles that went into the average shown here indicates that all are much closer to each other than any is to the lidar profile, with a spread of no more than ∼8 K at levels between 0.1 and 0.01 hPa. That, and the consistency of MLS with SABER, suggest that the deficiency may lie in the lidar profile at the highest levels. The appearance of similar differences between satellite and lidar profiles at other times when the stratopause is very high (thus, the 60–80 km altitude region is much warmer than climatology) (e.g., Fig. 7, 22 February 2004), and the likely impact of the initial temperature seed (Sect. 2.1), suggest that the initialization is "pulling" the top of many lidar profiles toward artificially low temperature in 2004 and 2006. Sica et al. (2007)[2] show that in 2004 and 2006, the Eureka Lidar is substantially colder than ACE-FTS in seasonal averages above ∼50 km, whereas in 2005 (when the lower mesosphere was colder than usual because of mesospheric cooling associated with the early stratospheric final warming), it is warmer. Examination of SABER temperatures at Eureka shows temperatures near 250–260 K at 70 km on the days of most lidar measurements in those years (thus, 30–40 K higher than the seed); a few days with lidar measurements in 2005 have 70-km SABER temperatures near the seed value of 220 K, but most are closer to 190–200 K, thus substantially lower than the seed. All of this is consistent with the influence of a seed value that is quite different from the local temperatures due to the extreme conditions during these winters.

3.4 Comparisons with Eureka radiosonde

Focusing now on the middle and lower stratosphere, Fig. 12 shows timeseries during the 2005 and 2006 Eureka campaigns of temperatures from the 11:15 UT daily radiosonde launches, compared with those from MLS and GEOS-4. We again see the

strong contrast between the two types of extreme winters: The temperature minimum is between 100 and 20 hPa in 2005, with the onset of the early final warming in mid-March indicated by the abrupt temperature increase just before 15 March 2005. In contrast, wintertime conditions in 2006 persisted throughout the campaign, but with a temperature minimum above 3 hPa at the start of the campaign, dropping to ∼10 hPa (∼30 km) by mid-March 2006. Because the daily operational radiosonde data are used in the meteorological analyses, it is no surprise that the GEOS-4 analyses (and the others, see below) agree very well with the radiosonde data below ∼25–30 km, with differences in detail reflecting the extremely fine vertical resolution of the radiosondes. GEOS-4, however, appears to overestimate the coldpoint altitude and underestimate its temperature compared to MLS and radiosondes after mid-March 2006. MLS, radiosonde, and GEOS-4 temperature time evolution and vertical structure agrees well, but MLS show a slight low bias with respect to radiosondes and a slight high bias with respect to GEOS-4 near the coldpoint, consistent with Schwartz et al. (2007)[5].

Figure 13 shows radiosonde profiles compared with ACE-FTS, MLS, SABER, and the meteorological analyses on three days in each of the three years chosen to illustrate changes during the campaigns and interannual differences. On 18 March 2006, the GEOS-4 profile shows a sharp temperature minimum just above 10 hPa, whereas radiosondes and MLS show a much shallower minimum just below 10 hPa, consistent with the behavior seen in Fig. 12. GEOS-5, ECMWF, and MetO follow the MLS and radiosonde profile more closely up to ∼6 hPa (top of the radiosonde profile). Similar behavior is apparent on 6 March 2006, but ACE-FTS and MLS both show vertical oscillations above ∼30 hPa, becoming more pronounced in the upper stratosphere. SABER shows no such oscillations. MLS (e.g., 23 February 2006) and ACE-FTS (e.g., 24 February 2005, 23 Feb 2006) show vertical oscillations on other days, and unphysical vertical oscillations have been reported in both MLS v2.2 (Schwartz et al., 2007[5]) and ACE-FTS v2.2 (Sica et al., 2007[2]). Some of the more egregious extrema in GEOS-4 are reduced or absent in GEOS-5, and generally are not seen in ECMWF or MetO (e.g., 6 and 18 March 2006 near 6 hPa).

Except for the previously noted oscillations in ACE-FTS and MLS, satellite observations agree well with radiosondes over the entire profiles. Since ACE-FTS temperatures are constrained to Canadian Meteorological Center analyses (which assimilate radiosonde observations) below 12 km, close agreement at the lowest levels is no surprise. MLS profiles are largely independent of radiosondes since profiles strongly influenced by the GEOS-5 a priori are excluded from comparisons by MLS quality-control screening.

The 24 February and 6 March 2005 profiles show a typical wintertime vortex structure, with 18 March 2005 showing temperature structure when the vortex is breaking up and has moved away from Eureka (Figs. 1, 2, 3). The profiles on all three days in 2004 and 2006, though sampled inside the vortex, are very atypical following the prolonged SSWs, as discussed above (Sect. 3.2).

3.5 MLS Trace Gases at Eureka

One of the important questions that arises from the disparate conditions in these three extreme winters is how these conditions affect transport in and around the polar vortex. Randall et al. (2005, 2006) showed unusually strong descent in the late winters of 2004 and 2006, with mesospheric air descending into the unusually strong vortex that reformed after the major SSWs in those years. Model simulations (Siskind et al., 2007) indicate the filtering of gravity waves by the disturbed stratospheric flow responsible for the very high altitude stratopause after the SSW also resulted in enhanced radiative cooling, not only making the upper stratosphere colder than usual and strengthening the redeveloping vortex, but also producing enhanced descent of mesospheric air into the upper stratospheric vortex. Unusual trace gas evolution may also be expected as a result of strong mixing of vortex and extra-vortex air during the SSWs. For measurements at Eureka, its position relative to the vortex also adds to the complexity of observed trace gas evolution. Numerous trace gas measurements were made during the Eureka campaigns (e.g. Walker et al., 2005; Kerzenmacher et al., 2005; Sung et al.,

2007a; Sung et al., 2007b[13]; Fraser et al., 2007[14]; Fu et al., 2007[15]), and their interpretation is facilitated by knowledge of the overall patterns of transport in the region. We use timeseries of MLS trace gas evolution at Eureka to illustrate how transport and chemical processes in the three winters control trace gas evolution at Eureka.

Figure 14 shows timeseries of the long-lived tracers CO, H_2O and N_2O from MLS v1.5 data coincident with Eureka during the 2004–2005 and 2005–2006 winters. As noted in Sect. 3.2, The position of the top of the sPV contours gives an indication of the location of the stratopause (Sect. 3.2), while the Eureka crossings of those contours in time show when the stratospheric vortex was over Eureka. The vortex was over Eureka during most of the 2004–2005 winter, and CO and H_2O show the signatures of strong, confined descent in the lower mesosphere through midstratosphere through late March (descending high CO/low H_2O contours). The vortex moved away from Eureka in early March 2005 at the beginning of the major final warming, but its remnants moved back over Eureka twice later in the month. During those periods, the high CO in the vortex over Eureka indicates that CO from the lower mesosphere descended well below 10 hPa (~30 km) over the course of the 2004-2005 winter, and the peak in H_2O mixing ratio, initially in the upper stratosphere, descended to ~40 hPa (~22 km). When the vortex was over Eureka during the 2005 campaign, that signature was seen in high CO, high H_2O below ~10 hPa, and very low N_2O. After ~10 March, the vortex had broken up above ~3–7 hPa and thus tracer values similar to those typical of midlatitudes

[13]Sung, K., Mittermeier, R. L., Strong, K., et al.: Partial and total column SFIT2 retrievals from Eureka DA8 spectra in spring 2004 and 2005, including comparisons with PARIS-IR and ACE Satellite measurements, Atmos. Chem. Phys. Discuss., in preparation, 2007b.

[14]Fraser, A., Goutail, F., Strong, K., et al.: UV-Visible measurements of ozone and NO_2 at PEARL, Eureka, Nunavut 2004-2007, Atmos. Chem. Phys. Discuss., in preparation, 2007.

[15]Fu, D., Mittermeier, R., Sung, K., Walker, K. A., Bernath, P. F., Fast, H., and Strong, K.: Simultaneous atmospheric remote sensing using Fourier transform Infrared spectrometers at Polar Environment Atmospheric Research Laboratory (PEARL) during spring 2006, Atmos. Chem. Phys. Discuss., in preparation, 2007.

were seen, since air from vortex remnants has been diluted by mixing with extravortex air (e.g. Manney et al., 2006a; Manney et al., 2007a[12]). Just before the middle of April, a brief period of low sPV and very high N_2O (low H_2O) shows the passage of a "frozen-in anticyclone" over Eureka in the early stages of its formation (Manney et al., 2006a, see Fig. 3).

In contrast, in 2005–2006, the signature of strong descent in CO and H_2O is interrupted by the SSW. The disappearance of that signature is not only because the vortex (or its remnant) moves away from Eureka, but also because the near-complete break up of the vortex resulted in extensive mixing of midlatitude and vortex air (e.g., Manney et al., "Satellite Observations and Modeling of Transport During the 2006 Major Stratospheric Sudden Warming", in preparation (M-SSW)). When the vortex moved back over Eureka in early February (at which point it was reforming only in the upper stratosphere), there is little indication of trace gas values similar to those in the vortex before the SSW. However, near the stratopause, as the vortex redeveloped, there was also strong descent from the lower mesosphere into the stratospheric vortex, in an echo of the behavior typical of the fall vortex development. Consistent with the arguments given above and the simulations of Siskind et al. (2007), this descent is much stronger than that at high altitudes in the 2005 late winter, when the upper stratospheric vortex was weakening and warming. The redeveloping vortex is over Eureka throughout the 2006 campaign, with corresponding evidence of enhanced descent. The lower "vortex edge" sPV contour indicates that the vortex had not redeveloped enough to be well-defined at lower altitudes; the descent of this contour over the course of the campaign, accompanied by that of vortex-like trace gas values, reflects the redevelopment of the vortex, while day-to-day variations indicate primarily changes in position of the vortex with respect to Eureka. As noted by M-SSW, the lower stratospheric vortex remained very weak and never redeveloped the strong tracer gradients across its edge that were seen before the SSW; thus N_2O (H_2O) below ~20 hPa during the campaign is considerably higher (lower) than those in the vortex before the warming.

Figure 15 shows similar timeseries of MLS v1.5 O_3, HCl and HNO_3 (the latter scaled

by 0.7 to correct a known bias in v1.5 MLS HNO_3 due to an error in a spectroscopy file, Santee et al., 2007b[9]), providing an overview of polar processing taking place over Eureka. The signature of descent in the vortex can be seen in these species through January 2005; the frozen-in anticyclone signature in April is also apparent. Strongly depressed gas-phase HNO_3 in late December through mid-February 2005 indicates polar stratospheric clouds (PSCs) observed by MLS over Eureka. Accompanying these, extremely low HCl in the vortex indicates extensive chlorine activation, as discussed in detail by Santee et al. (2007a)[16]. Chlorine was deactivated by the end of March 2005 (Santee et al., 2007a[16]). The motion of the vortex away from Eureka during the 2005 campaign is seen clearly in O_3 (HNO_3), in higher (lower) mixing ratios, and, when well outside the vortex in mid-March and after the vortex breakup, a higher altitude mixing-ratio peak (because extra-vortex air had not experienced confined descent). Transport signatures are less obvious in HCl because its horizontal gradients are weak in the NH middle and upper stratosphere, and the behavior in the lower stratosphere in 2005 is largely controlled by chemical processes.

In 2006, the major SSW and motion of the vortex away from Eureka are signaled in an abrupt increase (decrease) in O_3 (HNO_3) at levels around the mixing ratio peak, and a complete disappearance of downward trend of the contours that signifies confined descent. During the recovery and the Eureka campaign, the signature of strong descent and, in the lower stratosphere, vortex redevelopment, is apparent in all three species. While some chlorine activation is apparent over Eureka in early January, before the SSW reaches the lower stratosphere, deactivation was complete well before the beginning of the 2006 campaign.

[16] Santee, M. L., MacKenzie, I. A., Manney, G. L., et al.: A study of stratospheric chlorine partitioning based on new satellite measurements and modeling, J. Geophys. Res., submitted, available at http://mls.jpl.nasa.gov, 2007a.

4 ACE-FTS overview and MLS/SABER comparisons

ACE-FTS provided coverage of the high Arctic during the periods of interest here in February through March 2004, and January through March 2005 and 2006. ACE-FTS observations typically included both vortex and extra-vortex air (Figs. 1 through 3). We briefly summarize the conditions observed by ACE-FTS, and compare ACE-FTS trace gas evolution with that from MLS in 2004 and 2006. This overview demonstrates that the conditions we have described in detail over Eureka are characteristic of the high Arctic.

Figure 16 shows timeseries of ACE-FTS temperatures at latitudes above 60° N averaged over all measurements for each day, compared with daily averages of coincident measurements from MLS v2.2 and SABER. The top panels show the latitude and number of ACE-FTS profiles included on each day. Except on days with few ACE-FTS measurements, this is similar to a zonal mean with latitude varying from day to day, so shows average or characteristic high latitude conditions. ACE-FTS captured the main features of temperature evolution, with a low stratopause after the SSWs in 2004 and 2006 redeveloping at very high altitude, accompanied by an unusually high-altitude coldpoint. The 2005 stratopause remained near 50–60 km throughout the winter, with a coldpoint near 30–100 hPa. ACE-FTS temperatures show good quantitative agreement with MLS and SABER throughout the periods with coincident measurements. Sica et al. (2007)[2] show detailed quantitative comparisons of ACE-FTS, MLS, and SABER temperatures.

The evolution of CO and H_2O observed by ACE-FTS compared to coincident MLS v2.2 data is shown in Fig. 17. Because both vortex and extravortex values are included, the transport signatures are less distinct than those seen over Eureka. Nevertheless, the steady descent in January through March 2005 from the mesosphere to the mid-stratosphere, and the interruption of similar descent in January 2006 followed by a "replay" with enhanced descent from the mesosphere in February and March 2006 are clearly seen, as is the contrast between enhanced descent in late winter 2006 and

ACPD
7, 10235–10285, 2007

EGU

weak descent in late winter 2005. CO in the middle and upper stratosphere also shows the signature of mixing and vortex breakup during the SSW in late January 2006, in the dissipation of very high values characteristic of the vortex as they are mixed with midlatitude air with near-zero CO (M-SSW). ACE-FTS and coincident MLS CO and H_2O agree quite well, consistent with the results of Pumphrey et al. (2007)[10], Lambert et al. (2007)[6], and Manney et al. (2007a)[12]. Other ACE-FTS trace gases (not shown) also show evolution consistent with that discussed in Sect. 3.5.

5 Summary and conclusions

The winters of the first three Canadian Arctic ACE Validation Campaigns at Eureka ("Eureka campaigns") represented the two extremes of Arctic winter variability. New satellite datasets available during these winters from ACE-FTS, MLS, and SABER provide an unprecedented wealth of temperature and trace gas data covering the upper troposphere through the mesosphere. We have used ACE-FTS, MLS and SABER satellite data, along with meteorological analyses and high-resolution ground-based temperature data, to detail the dramatic contrasts in the meteorology during extremely cold and extremely disturbed Arctic winters, and relate these differences to variations in transport and chemistry. We focus on interpretation of conditions over Eureka to provide context for the validation campaigns, as well as showing how the extreme meteorology is reflected in ACE-FTS data.

There were unusually strong and prolonged major stratospheric sudden warmings (SSWs) in January in both 2004 and 2006. Temperature and vortex evolution was very similar in the two years, with the vortex breaking down throughout the stratosphere, reforming quickly in the upper stratosphere while remaining weak in the middle and (especially) lower stratosphere. In both years, the satellite data show that the stratopause (temperature maximum) reformed at very high altitude (near 80 km) during recovery from the SSWs. Because of model tops that are too low, lack of data constraints above the upper stratosphere, and inadequate gravity-wave parameterizations, the assimi-

lated meteorological analyses cannot capture these extreme stratopause variations. The 2004 and 2006 Eureka campaigns were during the recovery from the SSWs, with the redeveloping vortex over Eureka. Consistent with this, 2004 and 2006 temperatures at Eureka show a sharp, shallow, low tropopause near 400 hPa, a local temperature maximum near 200 hPa, decreasing temperatures up to ~10–3 hPa (where temperatures were as much as ~25 K below tropopause values in February to early March), and stratopause above 0.01 hPa, near 75–80 km.

In contrast, the 2005 winter was the coldest on record in the lower stratosphere, but with an early final warming/vortex breakup in mid-March; the upper stratospheric vortex began weakening and warming by February. At the start of the 2005 Eureka campaign, through early March 2005, the vortex was over Eureka, and temperature structure was typical of a cold winter vortex, with a weak tropopause near 200–300 hPa, coldpoint between ~100 and ~30 hPa, and the stratopause near 0.5–0.1 hPa. Upper stratospheric temperatures over Eureka were up to ~50 K lower in 2004 and 2006 (when a strong, cold vortex reformed after the SSW) than in 2005 (when the upper stratospheric vortex was already breaking down), while middle and lower stratospheric temperatures were up to ~20 K higher in 2004 and 2006 than in 2005. Timeseries of daily-average ACE-FTS and coincident MLS and SABER measurements, representing average high-latitude conditions, reflect similar temperature structure and evolution to that seen at Eureka.

Individual temperature profiles from the Eureka lidar show very good agreement with coincident MLS, ACE-FTS and SABER up to 50–60 km, with most differences in small vertical-scale structure consistent with the changing meteorological conditions around Eureka and the instruments' sampling patterns and resolution. When the stratopause was very high in 2004 and 2006, temperatures at the top of the lidar profiles were far above the value used for initialization there, while in 2005 they were often below that initial value; consistent with this, the temperatures from lidar near the top of the profiles were often lower (slightly higher) than the satellite temperatures in 2004 and 2006 (2005). Eureka radiosonde temperatures agree well with the satellite data and

the meteorological analyses, with differences related to disparate resolutions. ACE-FTS average high-latitude temperatures agree well with coincident MLS and SABER daily averages.

MLS trace gas distributions over Eureka highlight the effects of differing vortex conditions on transport and chemistry. Consistent with the strong, cold upper stratospheric vortex and the enhanced radiative cooling driving its redevelopment after the 2004 and 2006 SSWs, MLS CO and H_2O measurements show enhanced vortex descent over Eureka in 2006 compared to that in 2005 when the upper stratospheric vortex (and associated descent) was already weakening. Since the vortex was over Eureka during the 2006 campaign, whereas it was breaking up and moving away from Eureka during the 2005 campaign, MLS observed lower (higher) H_2O and CO (N_2O) near Eureka in 2005 than in 2006 in and above the middle stratosphere. Since the lower stratospheric vortex was warm and ill-defined in 2006, but over Eureka and still cold at the start of the 2005 campaign, N_2O (H_2O) at Eureka was low (high) in late February 2005 compared to the same time in 2006, and MLS HCl, HNO_3, and O_3 in 2005 showed continuing PSC activity, chlorine activation, and chemical O_3 loss. ACE-FTS high-latitude daily average trace gases, and coincident MLS values, show similar patterns.

The ACE-FTS, MLS and SABER datasets, along with high-resolution temperatures recorded during the Eureka campaigns, have allowed us to compare in detail the meteorology during these disparate winters, to demonstrate how these conditions affected transport and chemistry, and to provide a meteorological context for interpretation of measurements during the Canadian Arctic ACE Validation Campaigns.

Acknowledgements. We thank the MLS Science Team, especially R. P. Thurstans, R. Fuller, B. W. Knosp, B. J. Mills, D. T. Cuddy, C. Vuu, A. Mousessian, P. A. Wagner, and X. Sabounchi, and the ACE Science Team, especially S. McLeod, R. Skelton, and R. Hughes, for their continuing support and assistance. Thanks to GMAO and Steven Pawson for GEOS data and advice on their usage, the British Atmospheric Data Center for providing MetO data, and ECMWF for their products shown here. Research at the Jet Propulsion Laboratory, California Institute of Technology, is done under contract with the National Aeronautics and Space Administration. Funding for the ACE mission was provided primarily by the Canadian Space Agency and the

Natural Sciences and Engineering Research Council of Canada. The Canadian Arctic ACE Validation campaign project has been supported by the Canadian Space Agency (CSA), Environment Canada (EC), the Natural Sciences and Engineering Research Council (NSERC) of Canada, the Northern Scientific Training Program and the Centre for Global Change Science at the University of Toronto. Logistical and on-site technical support for the 2006 and 2007 campaigns was provided by the Canadian Network for the Detection of Atmospheric Change (CANDAC). CANDAC and PEARL are funded by the Canadian Foundation for Climate and Atmospheric Sciences, NSERC, the Canadian Foundation for Innovation, the Ontario Innovation Trust, the Ontario Ministry of Research and Innovation, and the Nova Scotia Research and Innovation Trust. Thanks to the staff of the Eureka Weather Station for the balloon launches and radiosonde data.

References

Barrett, B., Ricaud, P., Santee, M. L., et al.: Intercomparisons of Trace Gas Profiles from the Odin/SMR and Aura/MLS Limb Sounders, J. Geophys. Res., 111, D21302, doi:10.1029/2006JD007305, 2006, 2006. 10242

Bernath, B. F., McElroy, C. T., Abrams, M. C., et al.: Atmospheric Chemistry Experiment (ACE): mission overview, Geophys. Res. Lett., 32, L15S01, doi:10.1029/2005GL022386, 2005. 10237, 10240

Bloom, S. C., McElroy, C. T., Abrams, M. C., et al.: The Goddard Earth Observing Data Assimilation System, GEOS DAS Version 4.0.3: Documentation and Validation, Tech. Rep. 104606 V26, NASA, 2005. 10244

Boone, C. D., Nassar, R., Walker, K. A., Rochon, Y., McLeod, S. D., Rinsland, C. P., and Bernath, P. F.: Retrievals for the Atmospheric Chemistry Experiment Fourier-Transform Spectrometer, Appl. Opt., 44, 7218–7231, 2005. 10241

Braathen, G., Grunow, K., Kivi, R., Kyrö, E., Raffalski, U., Kopp, G., Urban, J., Hochschild, G., Goutail, F., Manney, G. L., Rösevall, J., and Murtagh, D.: Joint WMO/EU Arctic ozone bulletin, winter/spring summary, Tech. Rep. 2006-1, World Meteorological Organization/European Ozone Research Coordinating Unit, 2006. 10238

Carswell, A. I., Donovan, D. P., Bird, J. C., Duck, T. J., Pal, S. R., and Whiteway, J. A.: Measurements at the Eureka Arctic NDSC station with a Raman DIAL system, in: Advances in

atmospheric remote sensing with lidar, edited by Ansmann, A. and Neuber, R., pp. 521–524, Springer-Verlag, Berlin, 1996. 10239

Clerbaux, C., Coheur, P.-F., Hurtmans, D., Barret, B., Carleer, M., Semeniuk, K., McConnell, J. C., Boone, C., and Bernath, P.: Carbon monoxide distribution from the ACE-FTS solar occultation measurements, Geophys. Res. Lett., 32, L16S01, doi:10.1029/2005GL022394, 2005. 10241

Davies, T., Cullen, M. J. P., Malcolm, A. J., Mawson, M. H., Staniforth, A., White, A. A., and Wood, N.: A new dynamical core for the Met Office's global and regional modelling of the atmosphere, Q. J. R. Meteorol. Soc., 131, 1759–1782, 2005. 10245

Duck, T. J. and Greene, M. D.: High Arctic observations of mesospheric inversion layers, Geophys. Res. Lett., 31, L02105, doi:10.1029/2003GL018481, 2004. 10239

Dunkerton, T. J. and Delisi, D. P.: Evolution of potential vorticity in the winter stratosphere of January-February 1979, J. Geophys. Res., 91, 1199–1208, 1986. 10246

Froidevaux, L., Livesey, N. J., Read, W. G., et al.: Early Validation analyses of atmospheric profiles from EOS MLS on the Aura Satellite, IEEE Trans. Geosci. Remote Sens., 44, 1106–1121, 2006. 10241, 10242, 10250

Fussen, D., Vanhellemont, F., Dodion, J., Bingen, C., Walker, K. A., Boone, C. D., McLeod, S. D., and Bernath, P. F.: Initial intercomparison of ozone and nitrogen dioxide number density profiles retrieved by the ACE-FTS and GOMOS occultation experiments, Geophys. Res. Lett., 32, L16S02, doi:10.1029/2005GL022468, 2005. 10241

Gross, M. R., McGee, T. J., Ferrare, R. A., Singh, U. N., and Kimvilakani, P.: Temperature measurements made with a combined Rayleigh-Mie and Raman lidar, Applied Optics, 36, 5987–5995, 1997. 10239

Hauchecorne, A. and Chanin, M. L.: Density and temperature profiles obtained by lidar between 35 and 70 km, Geophys. Res. Lett., 8, 565–569, 1980. 10239

Highwood, E. J. and Berrisford, P.: Properties of the Arctic tropopause, Q. J. R. Meteorol. Soc., 126, 1515–1532, 2000. 10250

Hitchman, M. H., Gille, J. C., Rodgers, C. D., and Brasseur, G.: The separated polar stratopause: A gravity wave driven climatological feature, J. Atmos. Sci., 46, 410–422, 1989. 10248, 10249

Ivanov, A., Kats, A., Kurnosenko, S., Nash, N., and Zaitseva, N.: International Radiosonde Intercomparison Phase III (Dzhambul, USSR 1989) final report, Tech. Rep. WMO/TD-No. 451, World Meteorological Organization, Instruments and Observing Methods Report 40, 1991.

10240
Jin, J. J., Semeniuk, K., Jonsson, A. I., et al.: Co-located ACE-FTS and Odin/SMR stratospheric-mesospheric CO 2004 measurements and comparison with a GCM, Geophys. Res. Lett., 32, L15S03, doi:10.1029/2005GL022433, 2005. 10241
Kerzenmacher, T. E., Walker, K. A., Strong, K., et al.: Measurements of O_3, NO_2 and Temperature During the 2004 Canadian Arctic ACE Validation Campaign, Geophys. Res. Lett., 32, L16S07, doi:10.1029/2005GL023032, 2005. 10237, 10241, 10256
Kutepov, A., Feofilov, A., Marshall, B., Gordley, L., Pesnell, W., Goldberg, R., and Russell III, J.: SABER temperature observations in the summer polar mesosphere and lower thermosphere: Importance of accounting for the CO_2 ν_2 quanta V–V exchange, Geophys. Res. Lett., 33, L21809, doi:10.1029/2006GL026591, 2006. 10244
Labitzke, K.: Temperature changes in the mesosphere and stratosphere connected with circulation changes in winter, J. Atmos. Sci., 29, 756–766, 1972. 10248
Livesey, N. J., Read, W. J., Filipiak, M. J., et al.: MLS Version 1.5 Level 2 data quality and description document, Tech. Rep. JPL D-32381, Jet Propulsion Laboratory, 2005. 10242, 10243
Lorenc, A. C., Ballard, S. P., Bell, R. S., et al.: The Met. Office global three-dimensional variational data assimilation scheme, Q. J. R. Meteorol. Soc., 126, 2991–3012, 2000. 10244
Mahieu, E. and Fels, S. B.: Comparisons between ACE-FTS and ground-based measurements of stratospheric HCl and $ClONO_2$ loadings at northern latitudes, Geophys. Res. Lett., 32, L15S08, doi:10.1029/2005GL022396, 2005. 10241
Manney, G. L., Zurek, R. W., O'Neill, A., and Swinbank, R.: On the motion of air through the stratospheric polar vortex, J. Atmos. Sci., 51, 2973–2994, 1994. 10246
Manney, G. L., Krüger, K., Sabutis, J. L., Sena, S. A., and Pawson, S.: The remarkable 2003-2004 winter and other recent warm winters in the Arctic stratosphere since the late 1990s, J. Geophys. Res., 110, D04107, doi:10.1029/2004JD005367, 2005. 10237
Manney, G. L., Livesey, N. J., Jimenez, C. J., Pumphrey, H. C., Santee, M. L., MacKenzie, I. A., Froidevaux, L., and Waters, J. W.: EOS MLS observations of "frozen-in" anticyclonic air in Arctic summer, Geophys. Res. Lett., 33, L06810, doi:10.1029/2005GL025418, 2006a. 10258
Manney, G. L., Santee, M. L., Froidevaux, L., Hoppel, K., Livesey, N. J., and Waters, J. W.: EOS MLS observations of ozone loss in the 2004-2005 Arctic winter, Geophys. Res. Lett., 33, L04802, doi:10.1029/2005GL024494, 2006b. 10237, 10247

McHugh, M., Magill, B., Walker, K. A., Boone, C. D., Bernath, P. F., and Russell III, J. M.: Comparison of atmospheric retrievals from ACE and HALOE, Geophys. Res. Lett., 32, L15S10, doi:10.1029/2005GL022403, 2005. 10241

Mlynczak, M. and Russell, J.: An overview of the SABER experiment for the TIMED mission, NASA Langley Research Center, Optical Remote Sensing of the Atmosphere, 2, 5–7, 1995. 10243

Nash, J. and Schmidlin, F. J.: International Radiosonde Intercomparison (U.K., 1984, U.S.A., 1985) final report, Tech. Rep. WMO/TD-No. 195, World Meteorological Organization, Instruments and Observing Methods Report 30, 1987. 10240

Petelina, S. V., Llewellyn, E. J., Walker, K. A., Degenstein, D. A., Boone, C. D., Bernath, P. F., Haley, C. S., von Savigny, C., Lloyd, N. D., and Gattinger, R. L.: Validation of ACE-FTS stratospheric ozone profiles against Odin/OSIRIS measurements, Geophys. Res. Lett., 32, L15S06, doi:10.1029/2005GL022377, 2005. 10241

Randall, C. E., Harvey, V. L., Singleton, C. S., Bernath, P. F., Boone, C. D., and Kozyra, J. U.: Enhanced NO_x in 2006 linked to strong upper stratospheric Arctic vortex, Geophys. Res. Lett., 33, L18811, doi:10.1029/2006GL027160, 2006. 10256

Randall, C. E. , Harvey, V. L., Manney, G. L., et al.: Stratospheric effects of energetic particle precipitation in 2003–2004, Geophys. Res. Lett., 32, L05802, doi:10.1029/2004GL022003, 2005. 10256

Reichler, T., Dameris, M., and Sausen, R.: Determining the tropopause height from gridded data, Geophys. Res. Lett., 30, 2042, doi:10.1029/2003GL018240, 2003. 10250

Reinecker, M. M., Suarez, M. J., Todling, R., et al.: The GEOS-5 Data Assimilation System: A Documentation of GEOS-5.0, Tech. Rep. 104606 V27, NASA, 2007. 10244

Remsberg, E. E., Lingenfelser, G., Harvey, V. L., Grose, W., III, J. R., Mlynczak, M., Gordley, L., and Marshall, B. T.: On the verification of the quality of SABER temperature, geopotential height, and wind fields by comparison with Met Office assimilated anylyses, J. Geophys. Res., 108, 4628, doi:10.1029/2003JD003720, 2003. 10243

Remsberg, E. E., Deaver, L., Wells, J. , et al.: An assessment of the quality of HALOE temperature profiles in the mesosphere based on comparisons with Rayleigh backscatter lidar and inflatable falling sphere measurements, J. Geophys. Res., 107, 4447, doi:10.1029/2001JD001521, 2002. 10243

Schoeberl, M. R.: Extratropical stratosphere-troposphere mass exchange, J. Geophys. Res., 109, D13303, doi:10.1029/2004JD004525, 2004. 10250

Simmons, A. J., Hortal, M., Kelly, G., McNally, A., Untch, A., and Uppala, S.: ECMWF analyses and forecasts of stratospheric winter polar vortex break-up: September 2002 in the southern hemisphere and related events, J. Atmos. Sci., 62, 668–689, 2005. 10245

Siskind, D. E., , Eckermann, S. D., Coy, L., and McCormack, J. P.: On recent interannual variability of the Arctic winter mesosphere: Implications for tracer descent, Geophys. Res. Lett., 34, L09806, doi:10.1029/2007GL029293, 2007. 10249, 10256, 10258

Sung, K., Skelton, R., Walker, K. A., Boone, C. D., Fu, D., and Bernath, P. F.: N_2O and O_3 Arctic column amounts from PARIS-IR observations: Retrievals, characterization and error analysis, J. Quant. Spectrosc. Rad. Transfer, in press, 2007, 2007a. 10256

Swinbank, R. and O'Neill, A.: A stratosphere-troposphere data assimilation system, Mon. Weather Rev., 122, 686–702, 1994. 10244

Swinbank, R., Ingleby, N. B., Boorman, P. M., and Renshaw, R. J.: A 3D variational data assimilation system for the stratosphere and troposphere, Tech. Rep. 71, Met Office Numerical Weather Prediction Forecasting Research Scientific Paper, 2002. 10245

Swinbank, R., Keil, M., Jackson, D. R., and Scaife, A. A.: Stratospheric Data Assimilation at the Met Office - progress and plans, in: ECMWF workshop on Modelling and Assimilation for the Stratosphere and Tropopause 23-26-June, 2003, ECMWF, 2004. 10245

Untch, A., Miller, M., Hortal, M., Buizza, R., and Janssen, P.: Towards a global meso-scale model: The high resolution system T799L91 and T399L62 EPS, ECMWF Newsletter, 108, 6–13, 2006. 10245

Walker, K. A., Randall, C. E., Trepte, C. R., Boone, C. D., and Bernath, P. F.: Initial validation comparisons for the Atmospheric Chemistry Experiment (ACE), Geophys. Res. Lett., 32, L16S04, doi:10.1029/2005GL022 388, 2005. 10237, 10241, 10256

Waters, J. W., Froidevaux, L., Harwood, R. S., et al.: The Earth Observing System Microwave Limb Sounder (EOS MLS) on the Aura satellite, IEEE Trans. Geosci. Remote Sens., 44, 1075–1092, 2006. 10241

WMO: Scientific assessment of stratospheric ozone depletion: 2006, U. N. Environ. Program, Geneva, Switzerland, 2007. 10237, 10238

Wu, W.-S., Purser, R. J., and Parish, D. F.: Three-dimensional variational analyses with spatially inhomogeneous covariances, Mon. Weather Rev., 130, 2905–2916, 2002. 10244

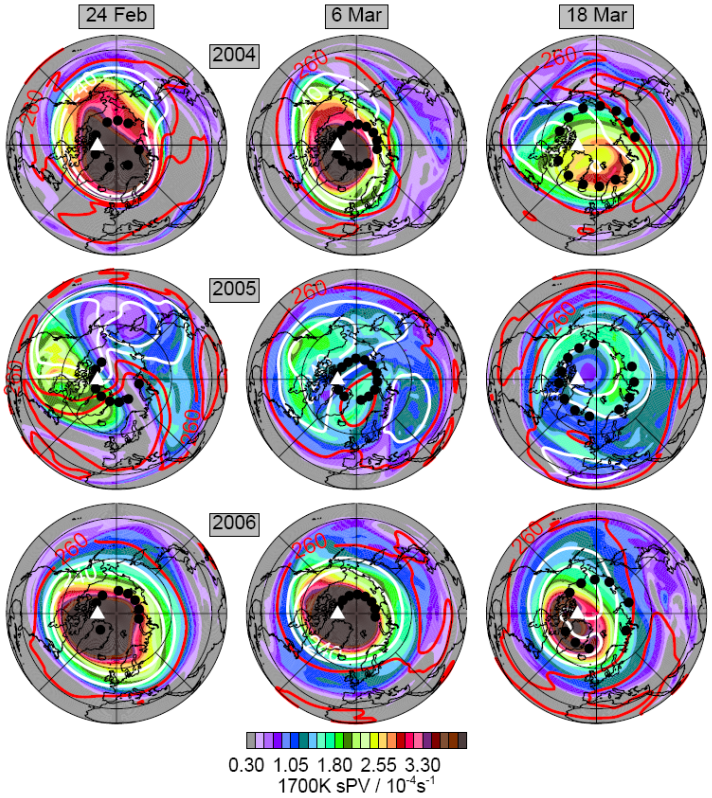

Fig. 1. Maps of scaled Potential Vorticity (sPV, $10^{-4}\,s^{-1}$) from GEOS-4 on the 1700 K isentropic surface (~1.5 hPa, ~50 km) on (left to right) 24 February, 6 March and 18 March in (top to bottom) 2004 through 2006. Contours are GEOS-4 temperatures of 240, 250, 260 and 270 K (lower two white, higher two red). Black dots show ACE-FTS observation locations and white triangle shows the location of Eureka. Projection is orthographic, from 0° to 90° N, with 0° longitude at the bottom and 90° E to the right.

ACPD
7, 10235–10285, 2007

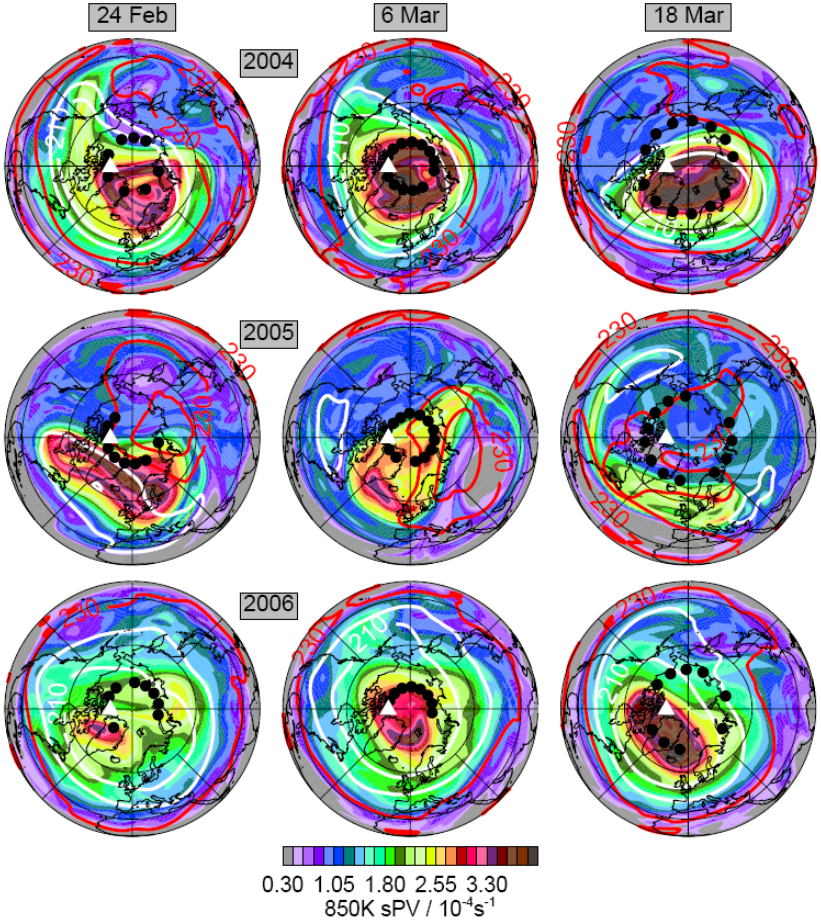

Fig. 2. As in Fig. 1, but at 850 K (~10 hPa, ~30 km), and with temperature overlays of 210, 220, 230 and 240 K (lower two white, higher two red).

ACPD
7, 10235–10285, 2007

EGU

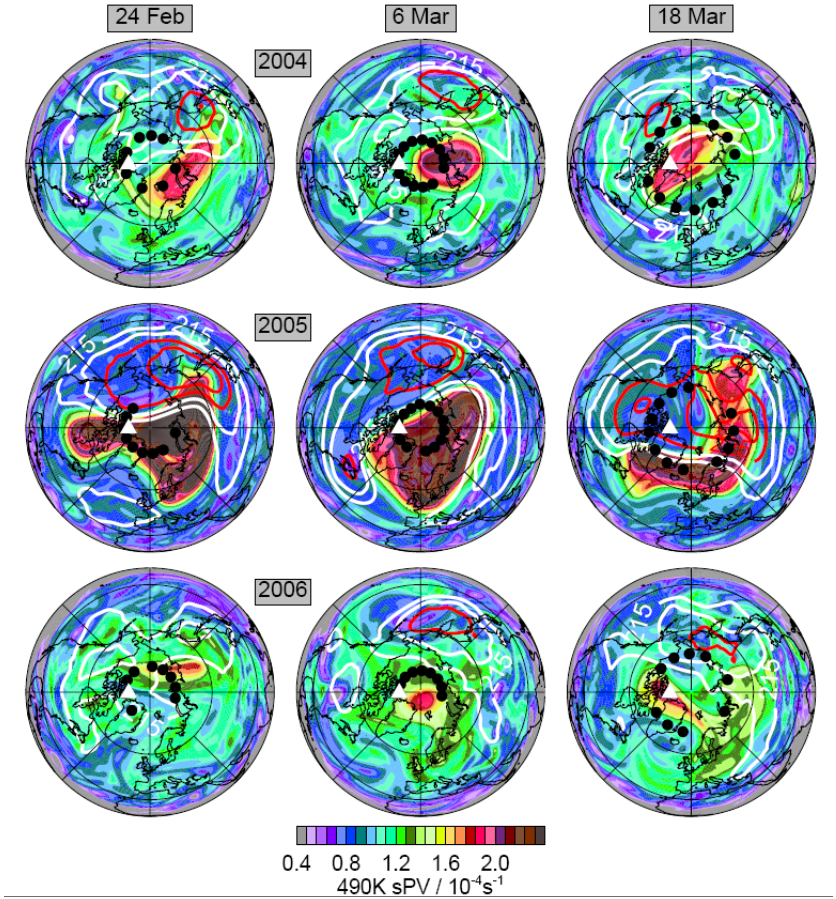

Fig. 3. As in Fig. 1, but at 490 K (~50 hPa, ~18 km), and with temperature overlays of 215, 220, 225 and 230 K (lower two white, higher two red).

ACPD
7, 10235–10285, 2007

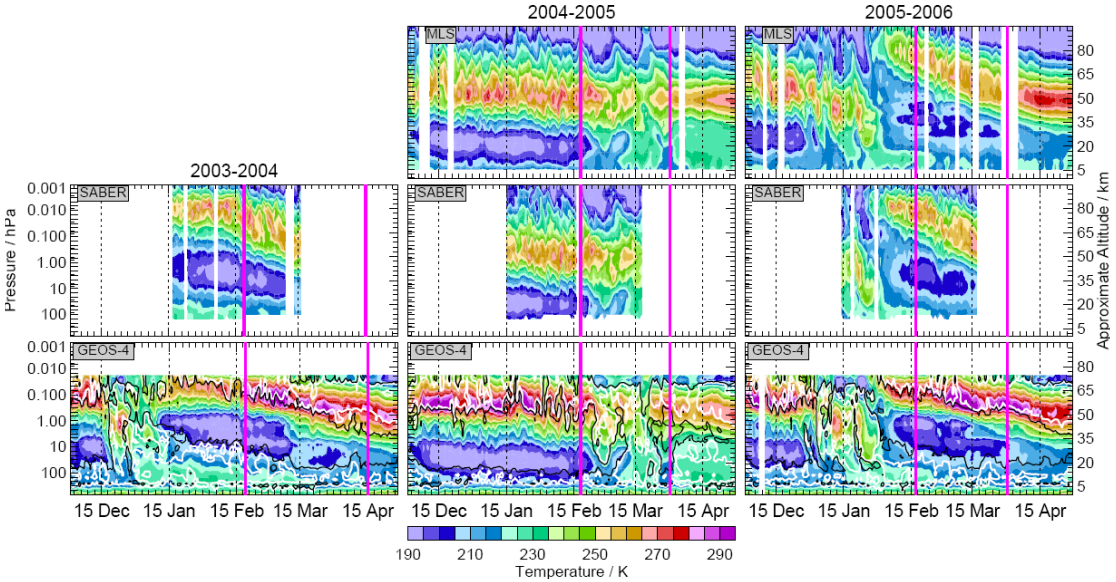

Fig. 4. Cross-sections of temperature (K) at Eureka as a function of time from December through April in (left to right) 2003–2004 through 2005–2006 from (top to bottom) MLS v1.5, SABER and GEOS-4. MLS and SABER temperatures are averages of all profiles within 2° latitude and 8° longitude of Eureka on each day; GEOS-4 values are bilinearly interpolated to Eureka's location. Overlays on GEOS-4 plots are 1.2 and $1.6\times10^{-4}\,s^{-1}$ sPV contours; these values are in vortex edge region in the stratosphere (see text), so going from white to black in time shows the vortex moving over Eureka, and black to white shows it moving away from Eureka. Magenta lines show periods of Eureka campaigns each year.

ACPD
7, 10235–10285, 2007

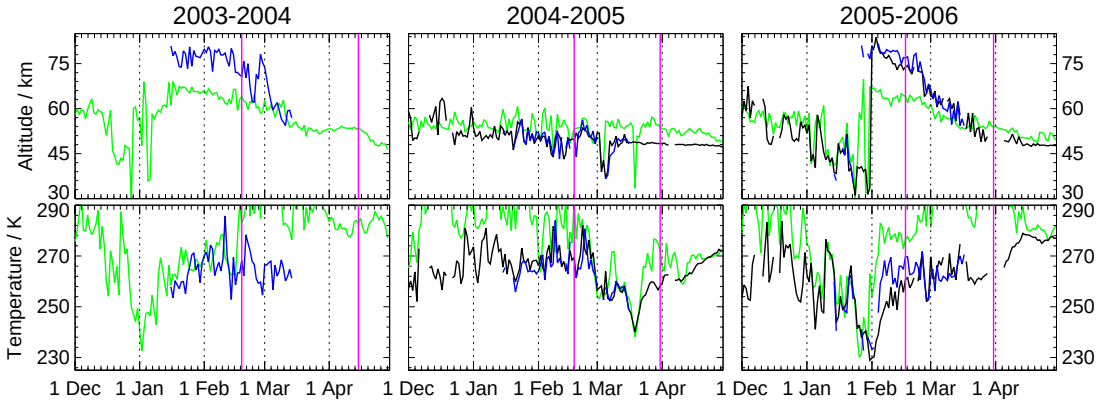

Fig. 5. Timeseries in (left to right) 2003–2004, 2004–2005 and 2005–2006 of MLS v1.5, SABER and GEOS-4 stratopause (top) altitude (km) and (bottom) temperature (K). MLS values are in black, SABER in blue, GEOS-4 in green. Magenta lines show periods of Eureka campaigns.

ACPD
7, 10235–10285, 2007

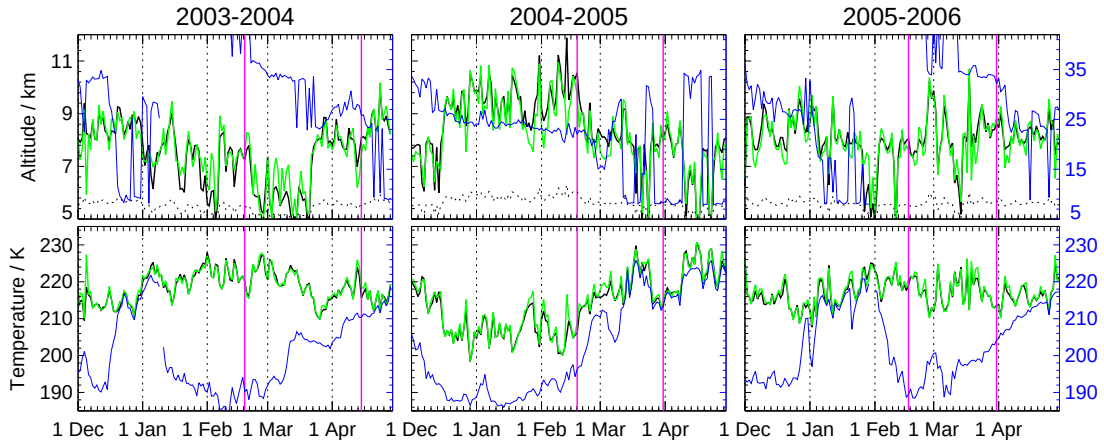

Fig. 6. Timeseries in (left to right) 2003–2004, 2004–2005 and 2005–2006 of GEOS-4 tropopause (top) altitude (km) and (bottom) temperature (K). Tropopause from WMO (temperature gradient) definition is in black, from dynamical definition (3.5 PVU) in green, and "coldpoint" value in blue. The left-hand y-axis scale is for WMO and dynamical definitions, right-hand scale for cold point (ranges are the same only for temperature). Magenta lines show periods of Eureka campaigns.

ACPD
7, 10235–10285, 2007

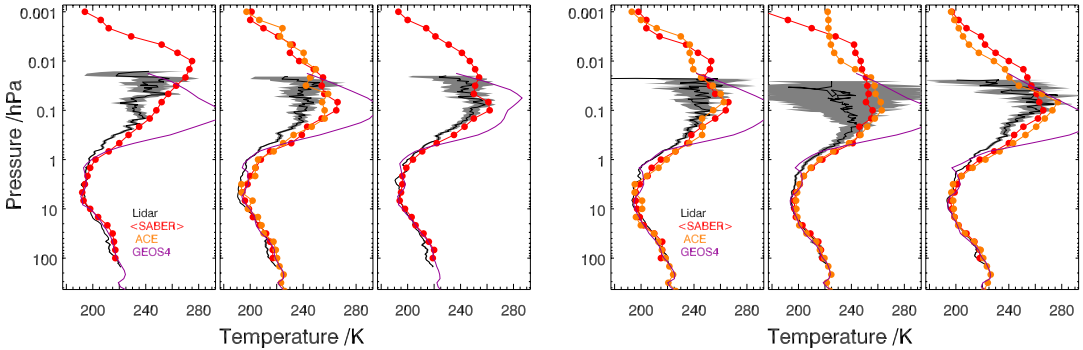

Fig. 7. Lidar profiles taken at Eureka on selected days in February and March 2004 compared with coincident profiles from SABER (red lines with dots), ACE (orange lines with dots), and GEOS-4 (purple lines without symbols). Lidar profile is in black, with 1-σ uncertainly range shown as grey shading.

ACPD
7, 10235–10285, 2007

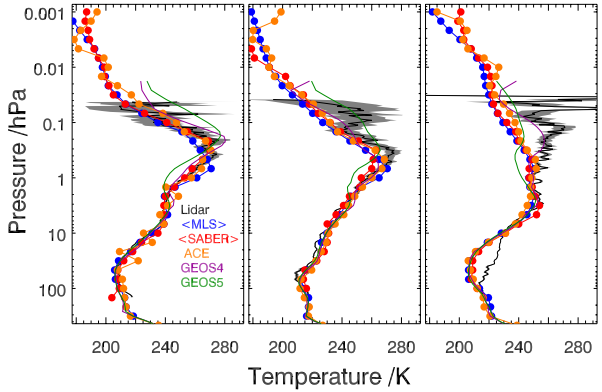

Fig. 8. As in Fig. 7, but during February and March 2005, and also showing MLS v2.2 (blue lines with dots) and GEOS-5 (dark green lines without symbols).

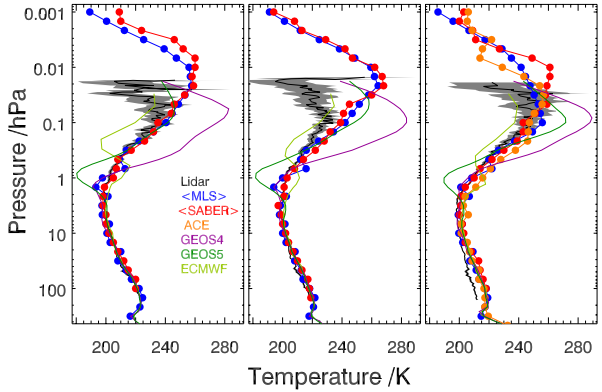

Fig. 9. As in Fig. 8, but for February 2006, and with ECMWF profiles (light green lines without symbols) added.

ACPD
7, 10235–10285, 2007

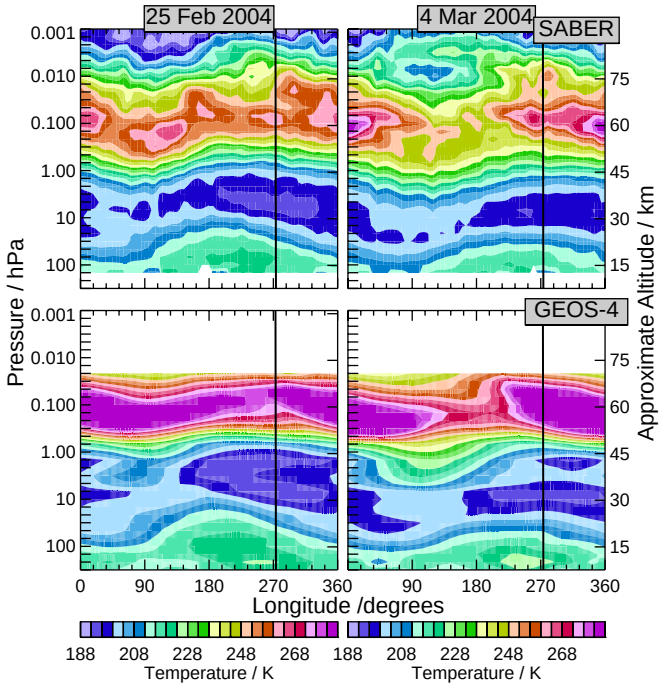

Fig. 10. Cross-sections of temperature from (top) SABER and (bottom) GEOS-4 around the 80° N latitude circle on (left) 25 February and 4 March 2004. Vertical black line is at longitude of Eureka.

ACPD
7, 10235–10285, 2007

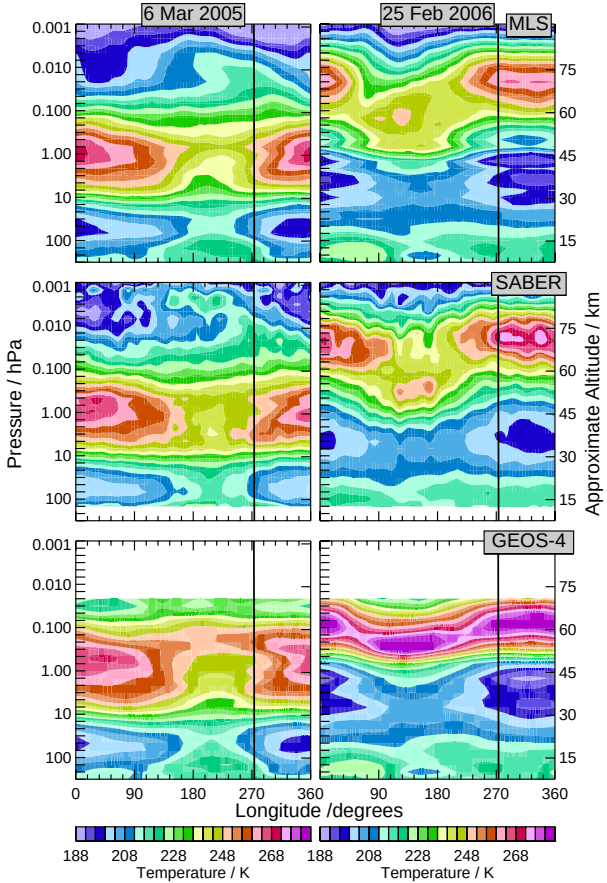

Fig. 11. As in Fig. 10, but for 6 March 2005 and 25 February 2006, and showing (top to bottom) MLS v2.2, SABER and GEOS-4 temperatures.

ACPD
7, 10235–10285, 2007

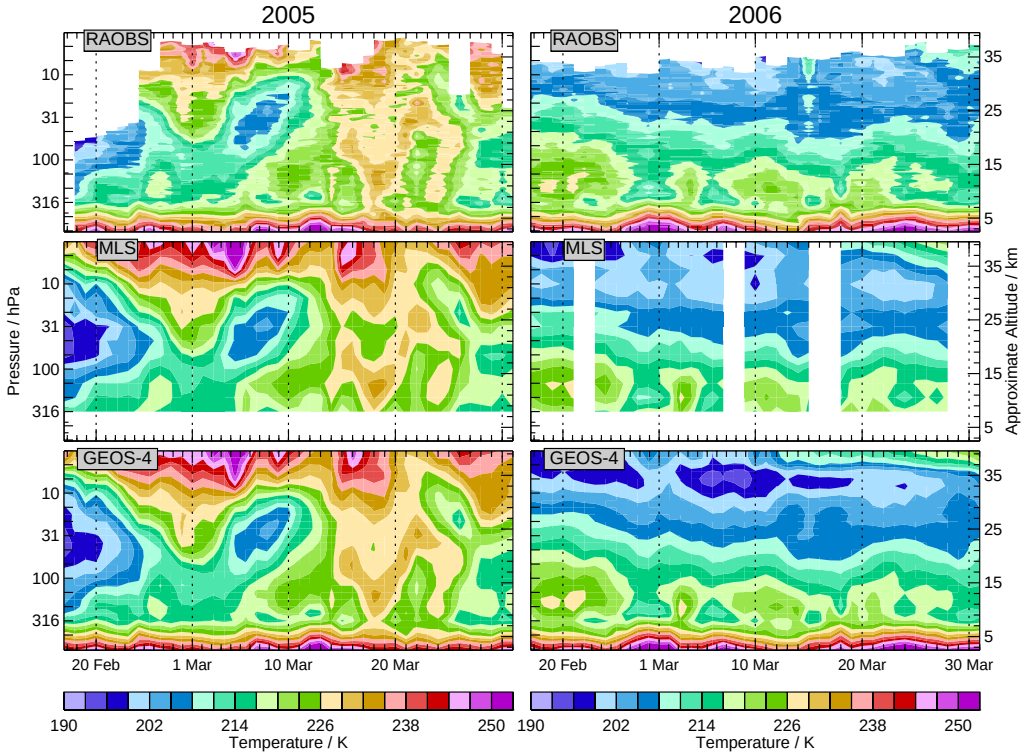

Fig. 12. Timeseries of (top) radiosonde temperatures during the (left) 2005 and (right) 2006 Eureka campaigns compared with (center) MLS v2.2 and (bottom) GEOS-4.

ACPD
7, 10235–10285, 2007

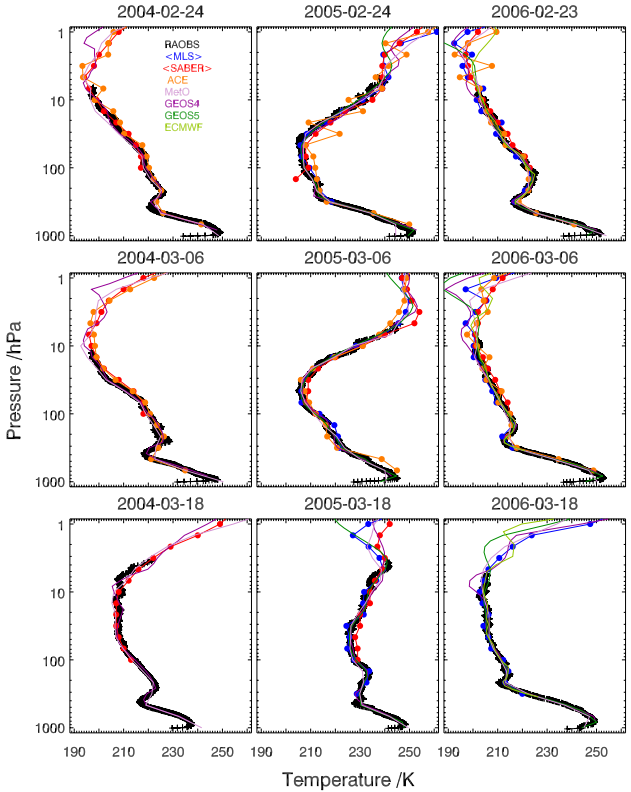

Fig. 13. Radiosonde profiles (black lines) at Eureka compared with MLS v2.2 (blue lines with dots), SABER (red lines with dots), ACE-FTS (orange lines with dots), GEOS-4 (purple lines), GEOS-5 (dark green lines), ECMWF (2006, light green lines), and MetO (light purple lines). Dates are (top to bottom) 24 February (23 February in 2006), 6 March, and 18 March in (left to right) 2004, 2005 and 2006.

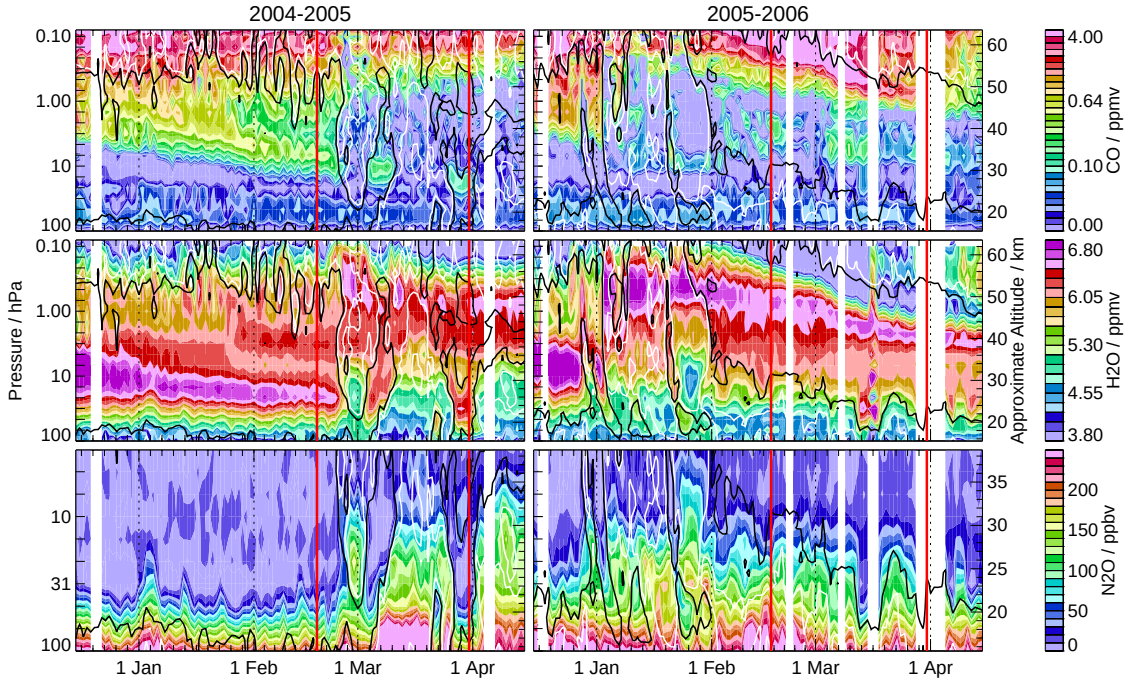

Fig. 14. Timeseries in (left) 2004–2005 and (right) 2005-2006 of v1.5 trace gas measurements from MLS near Eureka: (top) CO, (center) H_2O and (bottom) N_2O. Values on each day are averages of all observations coincident (see text) with Eureka on that day. Overlaid contours are sPV in the vortex edge region, with the black contour towards the vortex interior. Vertical magenta lines show periods of Eureka measurement campaigns. Vertical range for CO and H_2O is into the lower mesosphere; vertical range for N_2O is into the upper stratosphere.

ACPD
7, 10235–10285, 2007

EGU

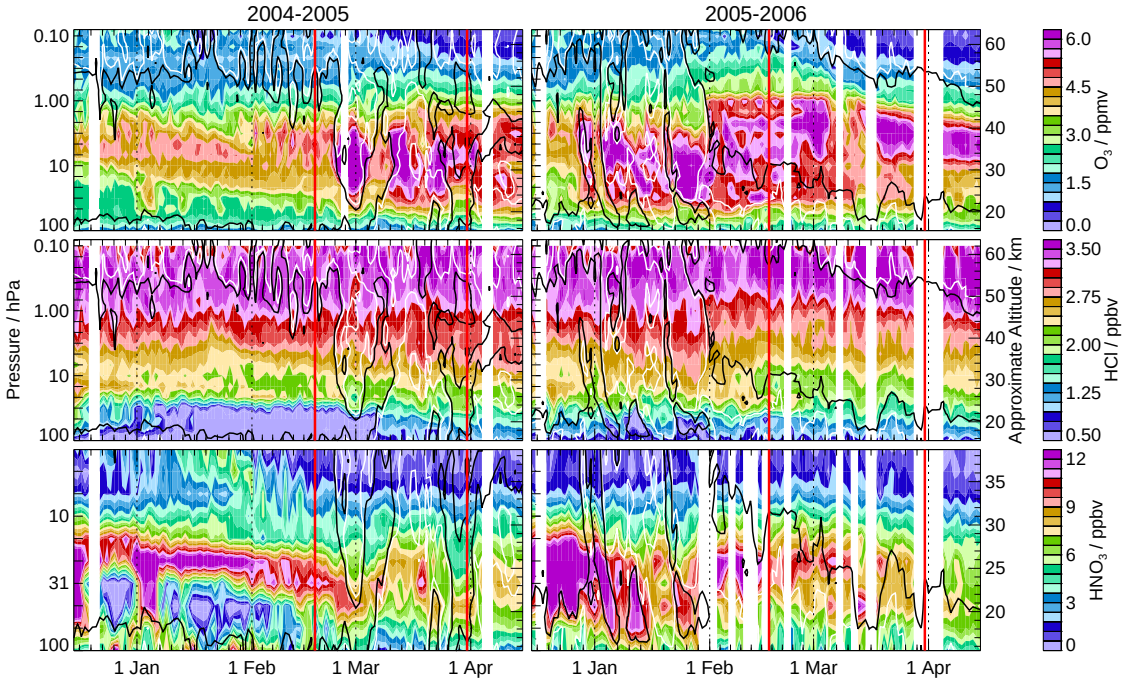

Fig. 15. As in Fig. 14, but for (top to bottom) MLS v1.5 O_3, HCl and HNO_3. Vertical range for O_3 and HCl is into the lower mesosphere; vertical range for HNO_3 is into the upper stratosphere.

ACPD
7, 10235–10285, 2007

EGU

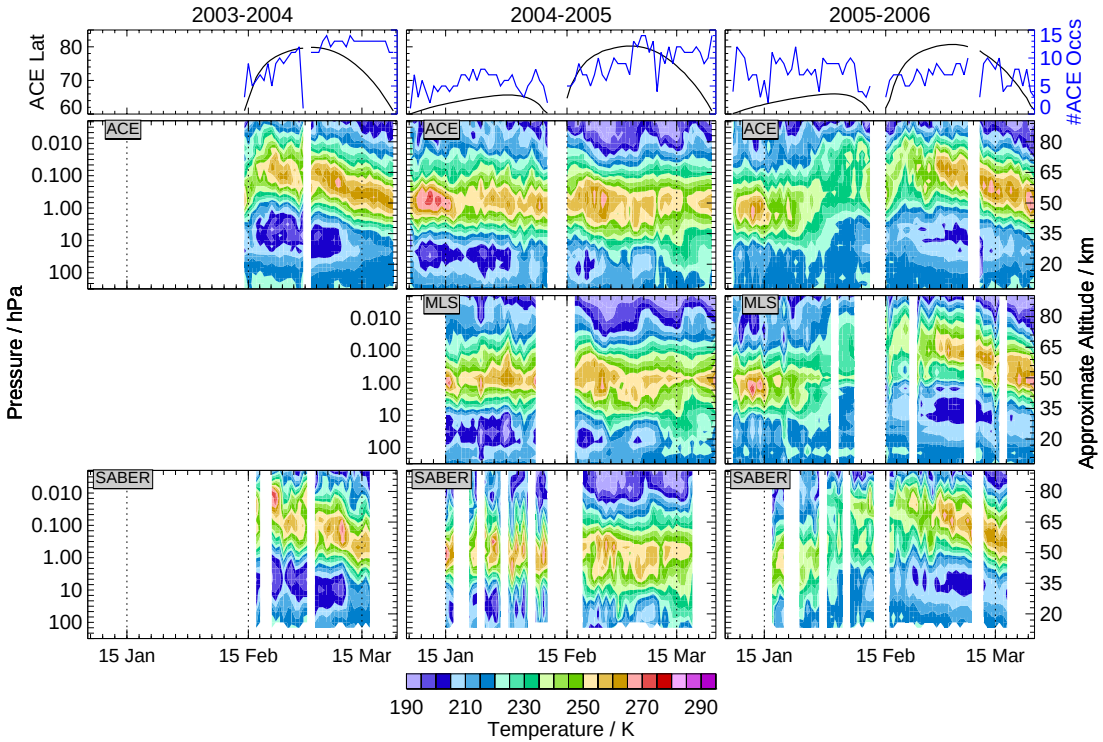

Fig. 16. Timeseries of temperatures (colored panels) from (top to bottom) ACE-FTS, MLS v2.2, and SABER. ACE-FTS values are the average of all occultations on each day north of 60° N; MLS and SABER values are averages of all observations coincident (see text) with the ACE-FTS observations used on each day. Top panels show average latitude of ACE-FTS observations (black), and number of ACE-FTS profiles included (blue) on each day. Time period covered is 5 January through 25 March in (left to right) 2004, 2005 and 2006.

ACPD
7, 10235–10285, 2007

EGU

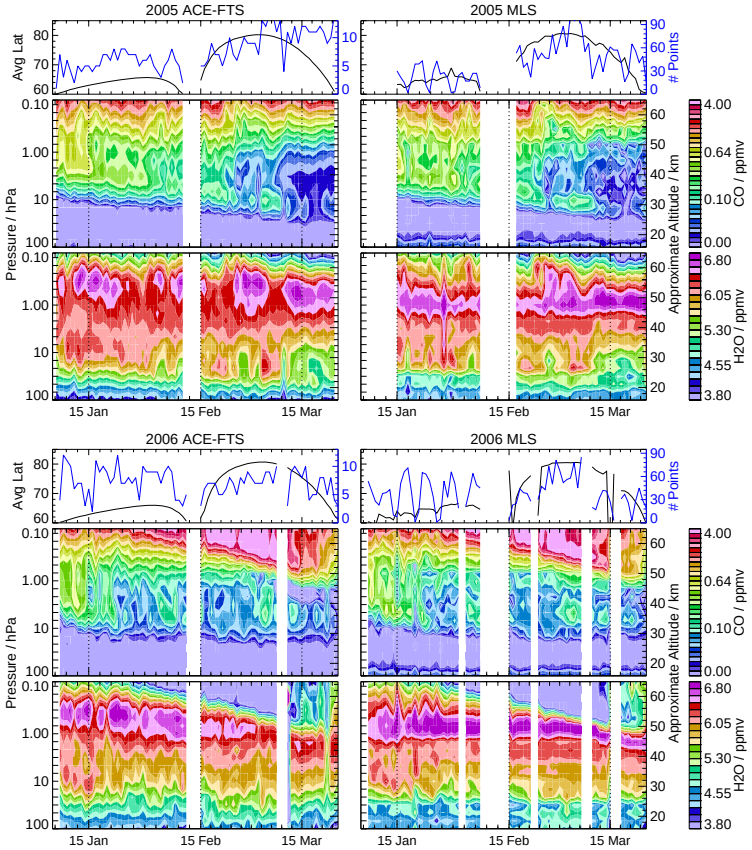

Fig. 17. Timeseries in (top set) 2005 and (bottom set) 2006 of ACE-FTS (left) and MLS v2.2 (top) CO and (bottom) H_2O. Averaging, coincidence criteria, and vertical ranges are as in Fig. 16. Top panels show average latitudes and number of profiles included for each instrument.

ACPD
7, 10235–10285, 2007

EGU